CHARACTERIZATION OF AVIAN REOVIRUS TEMPERATURE SENSITIVE MUTANTS

By

Wanhong Xu

A Thesis
Submitted to the Faculty of Graduate Studies
in Partial Fulfillment of the Requirements
for the Degree of

Master of Science

Department of Medical Microbiology and Infectious Diseases
University of Manitoba
Winnipeg, Manitoba
Canada

THE UNIVERSITY OF MANITOBA

FACULTY OF GRADUATE STUDIES

*****

COPYRIGHT PERMISSION PAGE

Characterization of Avian Reovirus Temperature Sensitive Mutants

BY

Wanhong Xu

A Thesis/Practicum submitted to the Faculty of Graduate Studies of The University of Manitoba in partial fulfillment of the requirements of the degree of

MASTER OF SCIENCE

TABLE OF CONTENTS

TABLE OF CONTENTS I

ACKOWLEDGEMENTS IV

LIST OF FIGURES V

LIST OF TABLES VII

LIST OF ABBREVIATIONS VIII

ABSTRACT 1

CHAPTER 1 INTRODUCTION 3

1.1 Avian reovirus 3

1.2 Virion structure and protein function 5

1.3 Avian reovirus lifecycle 9

1.3.1 Entry into cells 9

1.3.2 Transcription and replication 10

1.3.3 Assembly of progeny virions 13

1.3.4 Release 14

1.4 Reovirus genetics 15

1.4.1 Reassortment 15

1.4.2 Reassortant mapping 18

1.5 Temperature sensitive mutants 18

1.6 Objectives of this research 24

CHAPTER 2 MATERIALS AND METHODS 29

2.1 Stock viruses and cells 29

2.2 Viral manipulation 29

2.2.1 Virus passaging 29
2.2.2 Virus Plaque Assay 30
2.2.3 Virus purification 31
2.3 Virus growth curves 31
2.4 Determination of temperature sensitivity 32
2.5 Reassortant mapping 32
2.5.1 Generation of reassortants 32
2.5.2 Isolation of viral genome 33
2.5.3 Identification of reassortants by sodium dodecyl sulfate polyacrylamide gel electrophoresis (SDS-PAGE) 34
2.6 Electron microscopy of negative stained ARV particles 35
2.7 Sequencing the *tsA146* S2 gene 36
2.7.1 Viral RNA extraction 36
2.7.2 Primers 36
2.7.3 Reverse transcription and PCR amplification 36
2.7.4 Cycle sequencing 39
2.8 Placement of σA mutation within reovirus core crystal structure 40
2.9 Restriction endonuclease digestion 40
2.9.1 RT-PCR amplification of the M2 gene segment 40
2.9.2 Restriction enzyme analysis 41
2.10 Determination of the nucleotide sequence of the truncated S1 genome segment. 41
2.10.1 RT-PCR amplification of the S1 genome segment 41
2.10.2 Cycle sequencing 44

2.11 Statistical analysis 44

CHAPTER 3 RESULTS 45

3.1 Characterization of *tsA12* and *tsA146* 45

3.1.1 Comparison of replicative abilities of *tsA12*, *tsA146*, and ARV 138 45

3.1.2 Morphological analysis of *tsA12* and *tsA146* 46

3.1.3 Determination of localization of *ts* lesion in *tsA12* 53

3.1.4 Sequence analysis of the *tsA146* S2 gene 54

3.1.5 Structural locations of the mutations in *tsA12* and *tsA146* σA proteins 57

3.2 Determination of localization of *ts* lesion in *tsB31* 58

3.2.1 Identification of ARV176 × *tsB31* reassortants 58

3.2.2 Determination of temperature sensitivity of ARV176 × *tsB31* reassortants 61

3.2.3 Reassortant mapping of *tsB31* 64

3.3 Analysis of S1 gene truncation in some ARV clones 64

3.3.1 Electrophoretic analysis of viral RNA 66

3.3.2 Sequence analysis of the S1 genome segment 69

3.3.3 Identification of temperature sensitivity 73

3.3.4 Analysis of replicative ability 73

CHAPTER 4 DISCUSSION 76

4.1 Characterization of the group A mutants 76

4.2 S1 deletion mutants 80

4.3 Future directions 85

REFERENCES 88

ACKOWLEDGEMENTS

I would like to express my deeply thanks to my supervisor, Dr. Kevin Coombs for his help, guidance and support. Dr. Coombs leaves upon me a strong impression of a very kind and understanding person and a dedicated professor and researcher. I consider myself very fortunate for being given the opportunity to work on this project under his supervision.

I would like to thank all the past and present members of the Coombs lab: Megan Patrick, Laura Hermann, Magdalena Swanson, Israel Mendez, Paul Hazelton, Jieyuan Jiang, Archibald Nartey, Ita Hadžisejdić, Lindsay Noad, and Anh Tran. I am grateful for their help and friendship.

I wish to extend my gratitude to Dr. Paul Hazelton for his time, assistance, and guidance with the electron microscopy work. His invaluable contribution is very much appreciated.

I would like to thank my committee members Dr. Xi Yang and Dr. Elizabeth Worobec for their advice and encouragement.

Deeply thanks to my husband, Bingqing for giving me the endless love and creating the happiness in our life. Finally, I greatly thank my parents. Their unconditional love have been supporting and encouraging me all the time.

LIST OF FIGURES

Figure 1.1 Cartoon of avian reovirus genotype, protein profile, and composite particle. . 7

Figure 1.2 Co-infection and the generation of reassortant progeny. 17

Figure 1.3 Reassortant mapping. 20

Figure 1.4 Cartoon representing the plaque assay for a *ts* clone. 23

Figure 1.5 Model for mammalian reovirus assembly. 27

Figure 2.1 ARV 138 S1 segment sequence and the location of terminal primers. 43

Figure 3.1 Kinetics of viral growth in QM5 cells at various temperatures. 48

Figure 3.2 Graphical representation of the proportion of types of particles produced by ARV 138, *tsA12*, and *tsA146* at permissive and nonpermissive temperatures. 52

Figure 3.3 Alterations in deduced amino acid sequences of S2 gene product. 56

Figure 3.4 Locations of major σ core protein mutations of *tsA12* and *tsC447* in asymmetric unit of MRV core crystal structure. 60

Figure 3.5 Electropherotyping of ARV 138, ARV176, *tsB31*, and reassortants generated from an ARV 176 × *tsB31* co-infection. 62

Figure 3.6 Restriction profiles of the M2 gene segments of avian reovirus wild-type strain 176, mutant *tsB31*, and ARV 176 × *tsB31* reassortant clone 231. 63

Figure 3.7 Gene arrangement of the tricistronic S1 genome segment of avian reovirus. 67

Figure 3.8 Electrophoretic analysis of truncated segments from *ts31*× ARV 176 clones. 68

Figure 3.9 Agarose gel electrophoresis of PCR products produced by using full-length S1 genome segment target primers. 70

Figure 3.10 Alignment of the S1 segment cDNA sequences of ARV 138, ARV176, and 5 deletion mutants. 72

Figure 3.11 Growth curves of wild-type ARV 138 and 5 S1 deletion mutants. 75

Figure 4.1 Alterations in predicted amino acid sequences of MRV S2 gene product in corresponding wild-type and *ts* mutant. 79

Figure 4.2 Proposed reovirus assembly pathways. 81

LIST OF TABLES

Table 1.1 Genetic groupings and characteristics of avian reovirus temperature-sensitive mutants 25

Table 2.1 Oligonucleotide primers for RT-PCR amplification and sequencing of ARV S2 gene 37

Table 3.1 Distribution of types of particles produced by ARV138 and *tsA12* at permissive and nonpermissive temperatures[a] 50

Table 3.2 Electropherotypes and efficiency of plating (EOP) values of ARV176 × *tsA12* reassortants 55

Table 3.3 Identified mutations in *tsA146* S2 gene 56

Table 3.4 Electropherotypes and efficiency of plating (EOP) values of ARV176 × *tsB31* reassortants 65

Table 3.5 Efficiency of plating (EOP) values of S1 deletion mutants. 74

LIST OF ABBREVIATIONS

(-) RNA	minus sense ribonucleic acid
(+) RNA	plus sense ribonucleic acid
ARV	avian reovirus
BRV	baboon reovirus
cDNA	copy deoxyribonucleic acid
CPE	cytopathic effect
$CsCl_2$	cesium chloride
dATP	deoxyadenosine triphosphate
dCTP	deoxycytosine triphosphate
dGTP	deoxyguanosine triphosphate
DI	defective interfering
DMSO	dimethyl sulfoxide
DNA	deoxyribonucleic acid
dsRNA	double stranded ribonucleic acid
DOC	deoxycholate
DPI	days post infection
DTT	dithiothreitol
dTTP	deoxythymidine triphosphate
EDTA	ethylenediamine tetraacetate
EOP	efficiency of plating
FCS	fetal calf serum
HO	homogenization buffer
ISVP	intermediate/infectious subviral particle
$MgCl_2$	magnesium chloride
MOI	multiplicity of infection
mRNA	messenger ribonucleic acid
MRV	mammalian reovirus
NBV	nelson bay reovirus
NTPase	nucleoside triphosphate phosphohydrolase

PBS	phosphate buffered saline
PBS/EDTA	phosphate buffered saline/ethylenediamine tetraacetate
PCR	polymerase chain reaction
PFU	plaque forming unit
PI	post-infection
Px	passage (x = passage number)
RdRp	RNA dependent RNA polymerase
RNA	ribonucleic acid
RT	reverse transcription
SDS	sodium dodecyl sulfate
SDS-PAGE	sodium dodecyl sulfate polyacryamide gel electrophoresis
ssRNA	single stranded ribonucleic acid
TBE Buffer	tris/ boric acid/ EDTA buffer
ts	temperature sensitive

ABSTRACT

We have previously generated and described a set of avian reovirus (ARV) temperature sensitive (*ts*) mutants and assigned 11 of them to 7 of the 10 expected recombination groups, namely A, B, C...G (M. Patrick, R. Duncan, and K. M. Coombs, Virology 284:113-122, 2001). This study serves to further characterize group A mutants, *tsA12* and *tsA146*. The abilities of *tsA12* and *tsA146* to replicate at a variety of temperatures were determined. Morphological analyses of *tsA12* and *tsA146* were performed. Cells infected with the *tsA12* at nonpermissive temperature produced ~ 100-fold fewer particles and accumulated core particles. Cells infected with *tsA146* at nonpermissive temperature also produced ~ 100-fold fewer particles, of which a larger proportion were intact virions. The temperature sensitive lesion in *tsA12* was mapped to the S2 gene, which encodes major core protein σA. Amino acid alterations in the *tsA146* σA were determined. Analysis of the core crystal structure of the closely related mammalian reoviruses suggests that the mutated residue in ARV *tsA12* σA lies directly under the outer face of the σA protein. This may cause a perturbation in σA such that outer capsid proteins are incapable of condensing onto nascent cores. Thus, ARV mutant *tsA12* represents a novel orthoreovirus assembly-defective clone that may prove useful for delineating virus assembly. Analysis of the MRV core crystal structure also suggests that a mutated amino acid at position 290 in the *tsA146* σA is buried, where it seems to appear to affect interaction of σA with dsRNA, resulting in the shift in proportion of particles produced from top component to complete virions in restrictive infections.

The *ts* lesion of group B mutant, *tsB31* was localized to the M2 gene by reassortant analysis. In addition, 5 S1 deletion mutants which were generated from mixed

infection of wild-type ARV 176 and *tsB31* was identified and characterized. These deletion mutants originated from *tsB31* and thus were S1 deletion *ts* mutants. 5 S1 deletion fragments were sequenced. These fragments contained sequences from both termini of segment S1 and were 228- 230 nucleotides long. The consensus sequences consisted of 105- 119 nucleotides from the 5' end of the plus strand and 111- 123 nucleotides from the 3' end of the plus strand. It is concluded that these regions contain all the signals necessary for the replication and assembly of the S1 genome segment. The growth capacities of 5 S1 deletion mutants were examined at the permissive temperature of 33.5°C. Surprisingly, the infectious titers obtained from these mutants were 1- to 9-fold higher than that of wild-type ARV 138 at different times post-infection from 12 h to 84 h. This suggests that a novel mechanism might be involved in these S1 deletion mutants entry into the cells.

CHAPTER 1 INTRODUCTION

1.1 Avian reovirus

Avian reoviruses (ARV) are ubiquitous among poultry flocks. They are responsible for several diseases which cause considerable economic losses in poultry industry. They have been reported to cause tenosynovitis (arthritis) (Kibenege and Wilcox, 1983), which is the most important in chickens, a gastrointestinal maladsorption syndrome (Hieronymus *et al.*, 1983), and runting (Fahey and Crawley, 1954). The avian reoviruses have at least five serotypes by neutralization tests (Wickramasinghe *et al.*, 1993).

Avian reoviruses are members of the *Orthoreovirus* genus, one of the nine genera of *Reoviridae* family (Robertson and Wilcox, 1986; Nibert *et al.*, 1996). Members within the genus *Orthoreovirus* share similar capsid structures, genome segment profiles, and protein compositions (Nibert *et al.*, 2001). The orthoreoviruses consist of at least four species that separate into three subgroups (Duncan, 1999): subgroup 1 contains nonfusogenic mammalian reovirus (MRV) species; subgroup 2 contains the fusogenic avian reovirus and Nelson Bay reovirus (NBV) species; subgroup 3 is occupied by the single fusogenic baboon reovirus (BRV) species. Of these species, mammalian reoviruses, the prototype members of the *Orthoreovirus* genus, are most well-studied. The avian reoviruses, on the other hand, remain less well characterized at the molecular level than their mammalian counterparts. Like the mammalian reoviruses, the avian reoviruses are non-enveloped viruses and have a genome composed of 10 double-stranded RNA (dsRNA) segments that are enclosed within a double protein capsid shell

70-80 nm in diameter. The 10 RNA segments fall into 3 size classes by polyacrylamide gel electrophoresis (Figure 1.1A): 3 large segments (L1-L3), 3 medium segments (M1-M3), and 4 small segments (S1-S4). Homologous segments from different serotypes may exhibit differences in their electrophoretic mobilities. To date, the sequences of four S genome segments have been determined for some avian reovirus isolates, all of which posses a pentanucleotide UCAUC at the 3'-terminus of their plus strand (Shapouri *et al.*, 1995; Chiu and Lee, 1997; Yin *et al.*, 1997; Yin *et al.*, 2000) like in ten genome segments of mammalian reoviruses. For protein coding assignment of avian reoviruses, there is a good correlation between the sizes of the proteins observed in SDS-PAGE and the lengths of the corresponding genes for L and M encoded proteins, and the L and M genes appear to be monocistronic. Polypeptides encoded by the three L segments are denoted lambda (λ) A, λB, and λC; polypeptides by the M segments are named mu (μ)A, μB, and μNS. Of the S class genes, S1 codes for three proteins (p10, p17, and σC) from three partially overlapping open reading frames (ORFs), S2 codes for σA, S3 codes for σB, and S4 codes for σNS. Although avian and mammalian reoviruses have similar morphological and physicochemical characteristics, the avian reoviruses differ from their mammalian counterparts in their lack of hemagglutinin, the ability to induce cell fusion, and different host cell range (Wilcox *et al.*, 1982; Ni and Raming, 1993; Theophilos *et al.*, 1995). In spite of known knowledge of morphological and biochemical similarities of avian and mammalian reoviruses, the detailed understanding of molecular biology, structure/function and assembly of the avian reoviruses is lacking.

1.2 Virion structure and protein function

As described in the preceding section, avian reoviruses encode at least 12 translation products, 8 of which are structural proteins (λA, λB, λC, μA, μB, σA, σB and σC) (Figure 1.1B) and 4 of which are nonstructural proteins (μNS, σNS, p10, p17) (Varela and Benavente, 1994; Bodelon *et al.*, 2001). The knowledge of ARV structure is largely based on correlation to mammalian reovirus. The virion is proposed to be built from 8 structural proteins that are arranged in two concentric icosahedral capsid layers (Figure 1.1C) (Duncan, 1996; Van Regenmortel *et al.*, 2000; Reinisch *et al.*, 2000). The outer capsid layer is arranged with T = 13 icosahedral symmetry and the inner capsid layer has a T = 1 icosahedral symmetry. The outer capsid layer consists of three proteins (μB, σB and σC) and inner capsid layer (core) contains five proteins (λA, λB, λC, μA, σA). The locations of structural proteins within the virion are indicated in Figure 1.1C. The σB and μB are major outer capsid proteins. σB is the target for group-specific antibodies (Shapouri *et al.*, 1996). μB mainly presents as its cleavage product (μBc) in mature virion (Duncan, 1996). The μBc has been reported to have a role in virus entry and transcriptase activation (Duncan, 1996; O'Hara, 2001). Five monomers of λC form a pentameric complex (core spikes), extending from the inner core to the outer capsid at each of the 12 vertices (Martinez-Costas *et al.*, 1995; 1997). Biochemical studies have demonstrated that avian reoviruses contain all the enzymatic activities required for the synthesis of mature viral transcripts, and that the protein λC is the avian reovirus guanylyltransferase (Martinez-Costas *et al.*, 1995). Recent molecular analyses have suggested that λC may also have methyltransferase activity (Hsiao *et al.*, 2002). σC, the equivalent of the mammalian reovirus σ1 protein, is a minor component of outer capsid

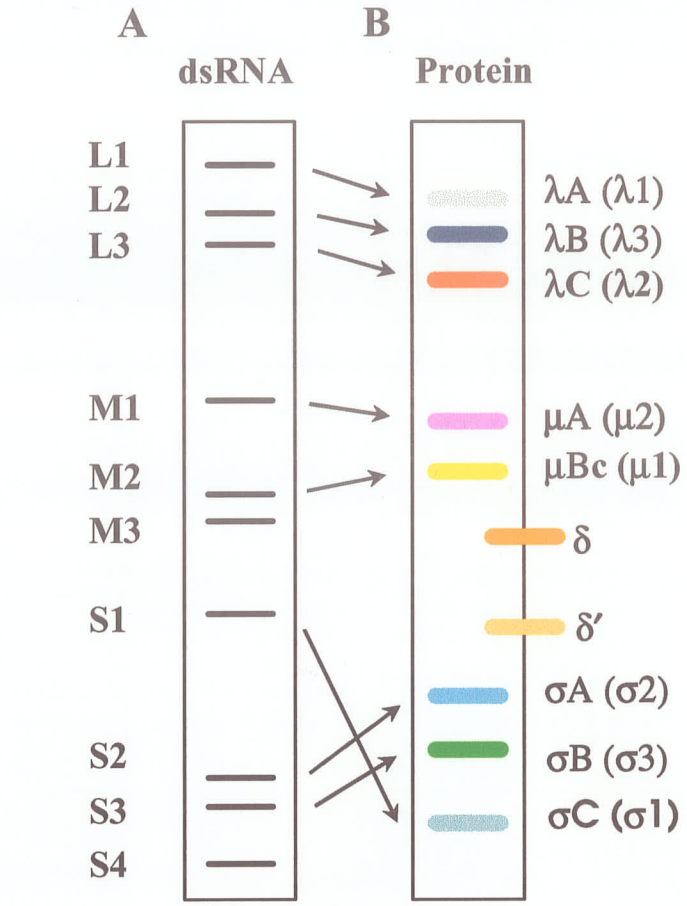
A
B
dsRNA
Protein
L1
L2
L3
M1
M2
M3
S1
S2
S3
S4
λA (λ1)
λB (λ3)
λC (λ2)
μA (μ2)
μBc (μ1)
δ
δ′
σA (σ2)
σB (σ3)
σC (σ1)

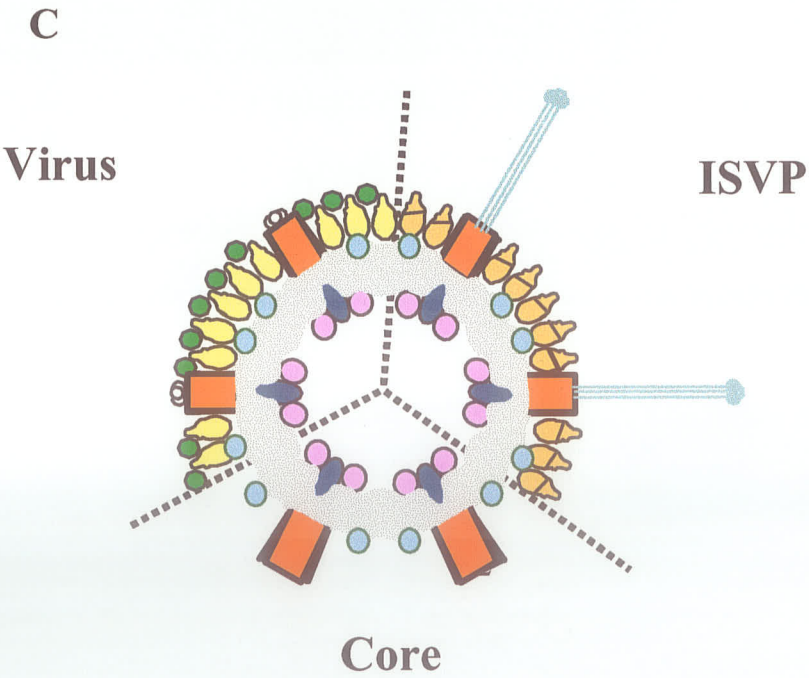
C
Virus
ISVP
Core

Figure 1.1 Cartoon of avian reovirus genotype, protein profile, and composite particle.

(A) The 10 dsRNA genome segments of avian reovirus strain 176 are separated on SDS-polyacrylamide gel. The genomic dsRNAs are grouped into three size classes referred to as large (L), medium (M), and small (S). (B) The structural proteins are designated in terms of their relative sizes and size classes. For an avian reovirus, these proteins are referred to as λA, λB, λC; μA, μB; σA, σB, σC. During the entry, μBc undergoes two distinct cleavages to generate δ and δ'. Proteins in parentheses indicate equivalent mammalian reovirus proteins. (C) The predicated locations of structural proteins are depicted in the three particle forms of reovirus: complete virus, ISVP (infectious or intermediate subviral particle) and core. Proteins are color coded to match the proteins in (B).

shell (Martinez-Costas *et al.*, 1997). In the intact virion, σC resides within the λC spike protein as folded trimers at the surface of each vertex (Theophilos, *et al.*, 1995). Protein σC has been identified as the cell-attachment protein (Shapouri *et al.*, 1996; Martinez-Costas *et al.*, 1997) and has also been associated with neutralization of virus infectivity (Wickramasinghe *et al.*, 1993; Theophilos *et al.*, 1995; Meanger *et al.*, 1999). Two of the S1-encoded products, σC and p10, have been suggested to display syncytium formation activity (Theophilos *et al.*, 1995; Meanger *et al.*, 1999; Shmulevitz and Duncan, 2000). However, recent evidence demonstrates that p10 but not σC is associated with cell-cell fusion (Bodelon *et al.*, 2001). λA is thought to form the shell of the core and σA binds on the outer surface of the λA shell. Protein λA is a dsRNA-binding protein (Yin *et al.*, 2000; Martinez-Costas *et al.*, 2000) and is also associated with nucleoside triphosphate phosphohydrolase (NTPase) activity (Yin *et al.*, 2002). λB and μA are internal core proteins. Protein λB is presumably located at the base of each of the 12 vertices and associated with protein μA.

Avian reoviruses have four morphological forms: virion, ISVP (infectious or intermediate subviral particle), core, and top component. Virions are intracellularly and/or extracellularly processed to generate ISVPs and cores. During conversion of virion to ISVP, σB is degraded; μBc is sequentially cleaved into δ and δ' (Duncan, 1996); and the σC fibres extend outwards. ISVPs can be further processed to cores with the loss of all μBc cleavage products and σC proteins. ISVPs and cores can also be generated by treating virions with proteases *in vitro*. ISVPs are infectious but not transcriptionally competent whereas cores are transcriptionally competent but not infectious, because of loss of the cell attachment protein. Top component structures account for a large

proportion of the particles lysed from infected cells. They remain similar protein content and morphology with those of full virions but lack the dsRNA genome; thus, their buoyant density is lower than that of complete virions. They are named as top component particles because they migrate above full virions in cesium chloride gradients.

1.3 Avian reovirus lifecycle

1.3.1 Entry into cells

Despite the widespread tissue dissemination of avian reovirus, the principal site of virus replication is the enteric tract (Kibenge *et al.*, 1985). The first step in reovirus infection is attachment of the virion (or ISVP) via cell attachment σC protein to host cell surface molecules (Theophilos *et al.*, 1995). Although receptor molecules for avian reoviruses have not been studied, evidence suggests that sialic acid, other sialoglycoproteins, EGF (epithelial growth factor) receptor, and the junction adhesion molecule are likely mammalian reovirus receptors (Gentsch and Hatfield 1984; Paul *et al.,* 1989; Choi *et al.,* 1990; Tang *et al.,* 1993; Barton *et al.,* 2001). Following attachment, virion or ISVP is internalized by receptor-mediated endocytosis. Alternatively, the ISVP is capable of directly penetrating the plasma membrane and bypassing the receptor mediated endocytosis entry pathway (Duncan, 1996). Once virions are adsorbed into endosomes, the endosomes will then fuse with lysosomes. The fusion of endosome with lysosome provides an acidic environment, which facilitates proteolytically processing of the virion or ISVP to core particle (Martinez-Costas *et al.*, 1997), a final proteolytic product released to the cytoplasm. It has been reported that ARV uptake is associated with sequential and two distinct cleavages of the major outer capsid protein μBc to δ and δ' (Duncan, 1996).

1.3.2 Transcription and replication

Contrary to mammalian reoviruses, the transcription and replication of avian reovirus have not been defined. However, evidence demonstrates that ARV possess all endogenous enzymatic activities required for the synthesis and maturation of viral transcripts, including a dsRNA-dependent RNA polymerase, a nucleoside triphosphate phosphohydrolase, an mRNA guanylytransferase and two mRNA methyltransferases (Martinez-Costas *et al.*, 1995). Of these, only guanylytransferase has been assigned to core spike protein λC (MRV λ2) (Martinez-Costas *et al.*, 1995). Avian reoviruses may resemble their mammalian counterparts in transcription and replication. Mammalian reovirus cores in the cytoplasm are transcriptionally active as they carry all enzymes for synthesis of mRNAs containing a type-1 cap at their 5' ends [$m^7G(5')ppp(5')G^mpCp...$] from each of their ten genomic stands (Faust *et al.*, 1975; Furuichi *et al.*, 1975). Several lines of evidence suggest that core protein λ3 (ARV λB) is the RNA-dependent RNA polymerase (RdRp) (Drayna and Fields, 1982a; Koonin *et al.*, 1989; Morozov, 1989; Starnes and Joklik, 1993) and μ2 (ARV μA) is the putative polymerase cofactor (Wiener *et al.*, 1989a; Yin *et al.*, 1996), all of which are the internal core proteins responsible for transcription and subsequent replication. Putative polymerase cofactor μ2 may further function as an NTPase (Noble and Nibert, 1997). Biochemical studies have identified that core spike protein λ2 (ARV λC) is a capping enzyme as it possesses guanylyltransferase activity (Shatkin *et al.*, 1983; Cleveland *et al.*, 1986; Mao and Joklik, 1991) and possibly methyltransferase activity (Seliger *et al.*, 1987; Reinisch *et al.*, 2000). Recent studies have demonstrated that core capsid protein λ1 (ARV λA) contains NTPase/helicase activity (Bisaillon *et al.*, 1997; Bisaillon and Lemay, 1997a), RNA 5'-triphosphatase

activity (Bisaillon and Lemay, 1997b), and can bind nucleic acids nonspecifically (Lemay and Danis 1994).

Replication and assembly of members of the *Reoviridae* family are thought to take place in viroplasms or viral factories. Mammalian reovirus or avian reovirus nonstructural protein μNS has been reported to form factory-like inclusions and recruits protein σNS to these structures (Becker *et al.*, 2003; Miller *et al.*, 2003; Touris-Otero *et al.*, 2004). The mammalian reovirus replication cycle is thought to have several steps: primary transcription, secondary transcription, and capsid assembly. Primary transcription is mediated by particles derived by partial uncoating of infecting particles (Chang and Zweerink, 1971; Silverstein *et al.*, 1972; Borsa *et al.*, 1981). Upon activation of the core, it begins synthesis of 10 nascent viral mRNAs from 10 minus strands of parental genome. These newly synthesized mRNAs undergo capping and methylation within the λ2 turrets and then are released via these λ2 channels to the cytosol (Gillies *et al.*, 1971, Bartlett *et al.*, 1974). It has been reported that transcripts from 4 genome segments (L1, M3, S3, and S4) are preferentially synthesized during the first several hours of infection (Watanabe *et al.*, 1968; Nonoyama *et al.* 1974; Spandidos *et al.*, 1976). The nascent primary transcription products are translated by cellular ribosomes to viral proteins, which associate with newly transcribed primary transcripts to form RNA assortment complexes. Assortment is likely to involve signals, possibly through short conserved regions at the 5' and 3' ends of each gene (Antczak *et al.,* 1982) that identify 10 distinct viral mRNAs to be packaged into replicase particles (Zou and Brown, 1992; Chapell *et al.,* 1994). For avian reoviruses, sequences have only been reported for S-class gene segments and L3 genome segment, all of which contain conserved terminal

sequences (Yin *et al.*, 2000; Hsiao *et al.*, 2002) that may serve as signals for packaging of corresponding plus strand RNAs. MRV σNS, as well as μNS and σ3, all have the capacity to bind ssRNA and may alone, or in cooperation, play a role in assortment (Huismans and Joklik, 1976; Antczak and Joklik, 1992). Likewise, ARV σNS has been identified to have ssRNA-binding activity, and thus may play similar role as does its cognate MRV σNS. Within the replicase particles, each of the 10 packaged plus strands serves as a template for minus-strand synthesis. Thus, the newly formed progeny subviral particles derived from those with replicase activity have a full complement of dsRNA, variable amounts of protein μNS, and reduced amounts of λ2 and the other outer capsid proteins (Morgan and Zweerink, 1975; Zweerink *et al.*, 1976; Skup and Millward, 1980). These progeny subviral particles trigger secondary transcription, which is the major source of the transcripts produced during infection (Ito and Joklik, 1972; Zarbl and Millward, 1983). These secondary transcripts are reportedly uncapped (Zweerink *et al.*, 1972; Morgan and Zweerink 1975; Zarbl *et al.,* 1980) and serve as the primary templates for viral protein synthesis at later times in infection. It is not known if these secondary transcripts are packaged and serve as templates for minus-strand synthesis. Furthermore, whether particles involved in secondary transcription can undergo subsequent assembly to form mature virions remain unknown.

During replication, both mammalian and avian reoviruses utilize a common mechanism to abolish the capacity of dsRNA to induce an innate host antiviral response, so that the translation of viral proteins can go on. MRV σ3 plays a crucial role in counteracting host antiviral action due to its dsRNA-binding activity (Imani and Jacobs, 1988). In contrast to mammalian reoviruses, avian reoviruses use a different protein, σA

(equivalent in MRV σ2) against host antiviral activity for survival. σA binds dsRNA and inhibits activation of the dsRNA-dependent enzymes (Martinez-Costas *et al.*, 2000; Gonzalez-Lopez *et al.*, 2003), thereby preventing interference of viral protein synthesis.

1.3.3 Assembly of progeny virions

The avian reovirus capsid assembly has not been described. Studies of mammalian reovirus assembly indicate that capsid assembly may involve the addition of preformed complexes of outer capsid proteins to core-like particles. Although detailed understanding of assembly is lacking, several lines of evidence suggest that MRV assembly may contain following stages. The earliest reovirus particles may be mRNA assortment complexes that primarily consist of major outer capsid protein σ3 and nonstructural proteins μNS and σNS (Gomatos *et al.* 1981; Antczak and Joklik, 1992). The next intermediate assembly particles are called RNase sensitive replicase particles, which contain an ssRNA-dependent dsRNA polymerase activity engaged in minus-strand synthesis, and both inner and outer capsid proteins, but lack nonstructural proteins (Acs *et al*, 1971; Morgan and Zweerink, 1975). These replicase particles become RNase resistant once the minus-strand RNAs are synthesized (Acs *et al*, 1971; Zarbl and Millward, 1983). Assembly is completed when additional copies of the outer capsid proteins are added to virion particles (Morgan and Zweerink, 1975; Zweerink and Morgan, 1976). Evidence also suggests that outer capsid protein complexes of μ1 (ARV μB) and σ3 (ARV σB) need to be preformed before they condense onto the core-like particles (Shing and Coombs, 1996). The σ1 (ARV σC) may self-assemble into oligomers and interacts with λ2 (λC) via its sequences near the amino terminus (Mah *et al.*, 1990; Leone *et al.*, 1991).

1.3.4 Release

The syncytium formation mediated by viral envelop glycoprotein(s) is a direct result of the mechanisms used by numerous enveloped viruses to enter and exit cells (White, 1990). Avian reovirus, Nelson Bay reovirus, and baboon reovirus represent a limited number of nonenveloped viruses that induce cell-cell fusion, resulting in multinucleated-syncytium formation. The syncytial phenotype mediated by fusion proteins have been defined as p10 in avian reoviruses and Nelson Bay reoviruses, and p15 in baboon reoviruses. These fusion proteins, so called FAST (fusion-associated small transmembrane) proteins are special in that they are not components of the virions but are small nonstructural proteins expressed in virus-infected cells and localized to the plasma membrane of these infected cells responsible for fusion of the infected cell with neighboring uninfected cells (Shmulevitz and Duncan, 2000; Dawe and Duncan, 2002). While enveloped virus-induced syncytium formation during the replication may significantly contribute to viral pathogenesis (Goodman and Engel, 1991; Sato *et al.*, 1992; Park *et al.*, 1994), avian reovirus-induced syncytium formation, however, is an independent event that occurs during replication cycle with almost no effect on the rate or extent of infectious progeny virus production, but it does enhance the rate for virus-induced cytopathology and virus egress (Duncan *et al.*, 1996). ARV progeny virions are released from infected cells following cell lysis, a process commonly associated with all noneveloped viruses.

1.4 Reovirus genetics

1.4.1 Reassortment

The segmented nature of reovirus genome allows genomes from different strains to undergo assortment during mixed infections, resulting in generation of progeny virions (reassortants) that contain a mixed set of gene segments from two parental strains (Ramig and Ward, 1991). Each strain genome possesses characteristic migration pattern upon polyacrylamide gel electrophoresis. For example, avian reovirus strains ARV138 and ARV176 are distinguishable under electrophoresis, because every homologous gene segment migrates at different rate. Thus, it is possible to identify parental origin of each gene segment in any reassortant when viewed in polyacrylamide gels.

If two strains that infect the same cell processed a completely random assortment, the resulting progeny would have 2^n (where n is the number of gene segments) possible gene combinations of genome segments from two parents. With 10 gene segments of reoviruses, in theory, there will be 2^{10} (1,024) different gene combinations, of which two are parental and the rest are reassortants (Figure 1.2). In practice, however, only a total of 3-25% progeny reassortants are produced from co-infection (Fields 1971). Precise understanding of these nonrandom segregation phenomena is lacking. However, two plausible explanations have been made. One is that the failure of efficient reassortments results from homologous RNA segments that need to be exchanged replicating in separate areas within an infected cell (Joklik and Roner, 1995). The second one is that viral RNAs and/or proteins from different parents may not interact effectively, so that potential reassortants could not survive (Roner *et al.,* 1990). In addition, evidence suggests that some genome segments or their protein products from two strains need

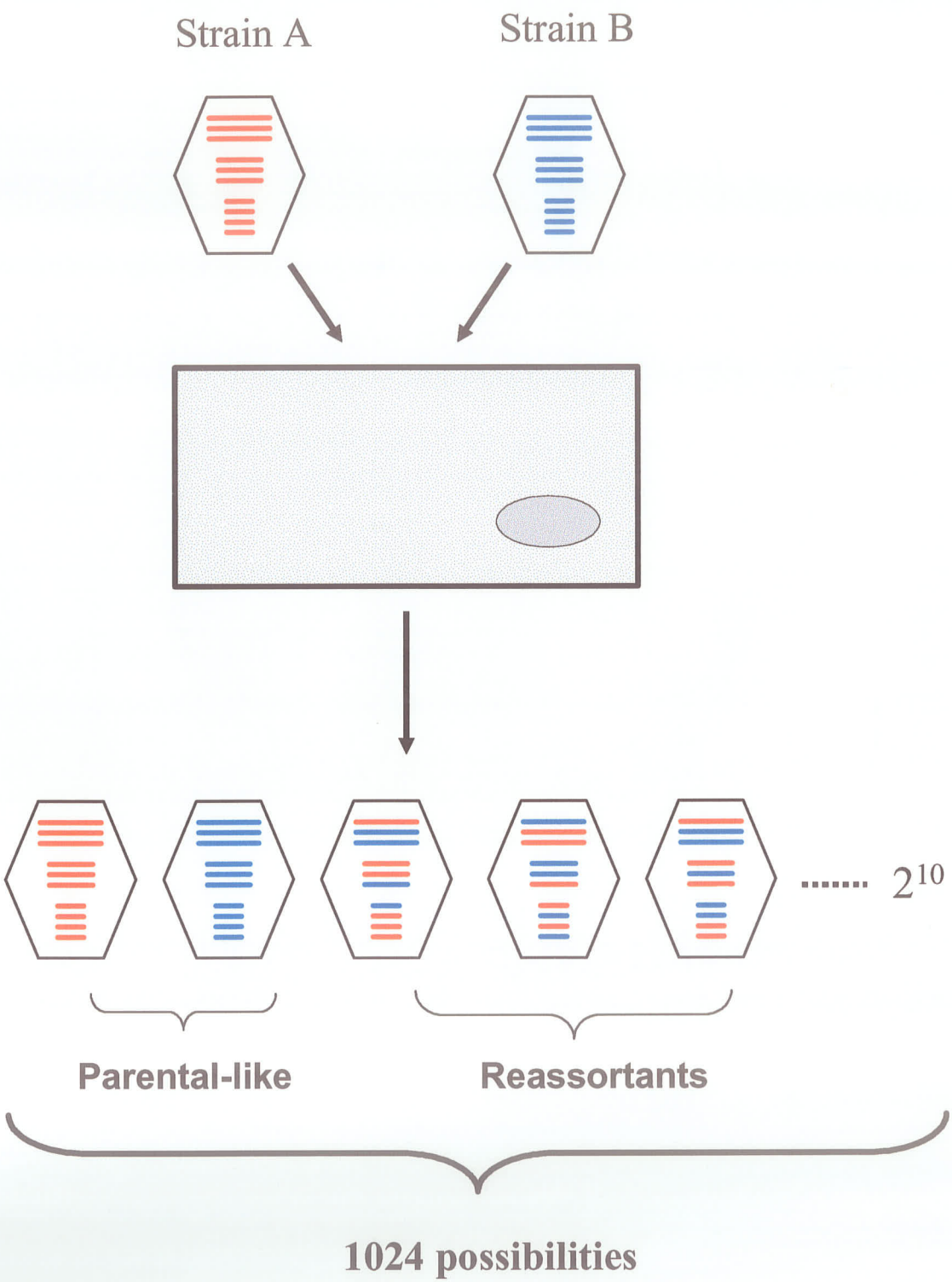
Strain A
Strain B
..... 2^{10}
Parental-like
Reassortants
1024 possibilities

Figure 1.2 Co-infection and the generation of reassortant progeny.

When two virus strains with segmented genomes infect the same cell, they may undergo genetic mixing to generate progeny viruses with hybrid gene segments. The process of the genetic mixing is called assortment and the progeny viruses with mixed gene segments are called reassortants. If assortment was a completely random process, with 10 gene segments of the viruses, one would expect to have 2^n (where n is number of gene segments) = 2^{10} (1024) possible gene combinations produced from the co-infection. Different viral serotypes have different electropherotypes, thus the origin of reassortant gene segments can be identified by SDS-PAGE.

accommodating mutations, so that they can be productively paired (Nibert *et al.*, 1996).

1.4.2 Reassortant mapping

If the two parental viral strains differ phenotypically, reassortment analysis of various reassortants in the same assay is useful for determining the gene(s) responsible for the phenotypic difference. For example, mutants can be mapped to individual RNA segments by performing intertypic crosses between virus types that differ in the electrophoretic mobility of each RNA segment. Specifically, if crosses are performed between a wild-type virus of one type and a mutant virus of another type and numerous wild-type progeny analyzed, one segment bearing the wild-type allele will be conserved among all the progeny, while all other segments will display reassortment. Such reassortant analysis is commonly termed reassortant mapping. For a schematic example, please see Figure 1.3. Because of monocistronic nature of virtually all gene segments, reovirus reassortments have served as a powerful tool for relating particular functions to specific viral proteins (For examples, see: Weiner *et al.*, 1980; Yin *et al.*, 1996; Sherry *et al.*, 1998; Becker *et al.*, 2001; O'Hara *et al.*, 2001).

1.5 Temperature sensitive mutants

Temperature sensitivity is a type of conditional lethality in which mutants can grow at a low, permissive temperature but not at a high, nonpermissive temperature, in contrast to wild-type virus, which grows at both temperatures. Temperature-sensitive (*ts*) mutants have proved enormously useful in all branches of virology, but they have been particularly useful for the study of animal viruses. The use of mammalian reovirus *ts*

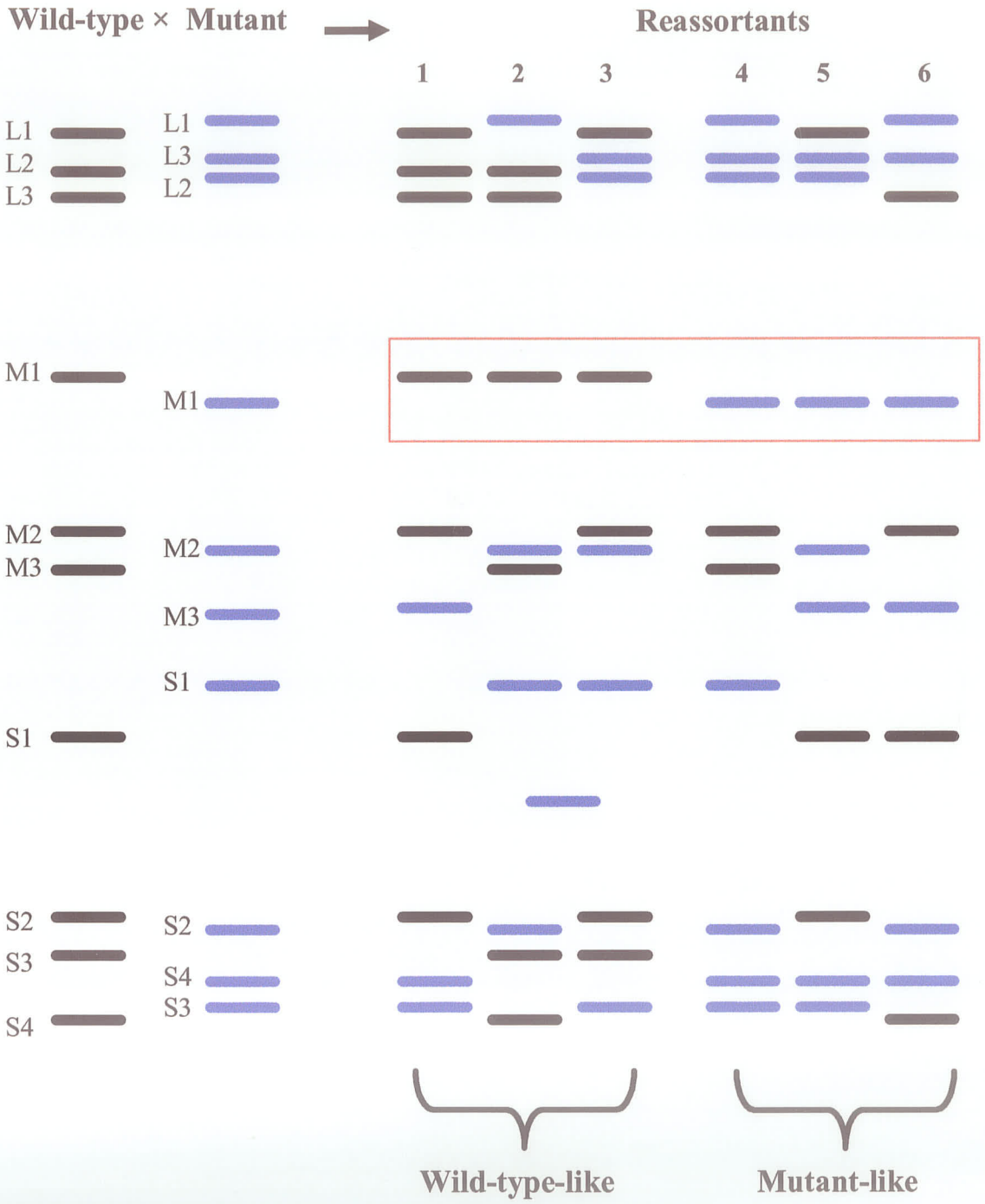
Wild-type × Mutant
Reassortants
1
2
3
4
5
6
L1
L2
L3
L1
L3
L2
M1
M1
M2
M3
M2
M3
S1
S1
S2
S3
S4
S2
S4
S3
Wild-type-like
Mutant-like

Figure 1.3 Reassortant mapping.

If the two parental viral strains differ phenotypically, reassortants generated from the two parents can be used to identify gene responsible for the response. In this example, reassortants were generated from a mixed infection of a wild-type ARV strain and a mutant virus of another type and their electropherotypes resolved by SDS-PAGE. Reassortants behaved like wild-type virus are indicated as 1, 2, and 3, respectively. Reassortants behaved like mutant under the same assay are indicated as 4, 5, and 6, respectively. Analyses of the electropherotypes of the reassortants indicate that the wild-type-like group all had their M1 gene segment derive from the wild-type virus whereas the mutant-like group all had their M1 gene segment come from the mutant. The other genome segments are randomly distributed. Thus, the M1 gene is mapped to be responsible for the phenotypic difference between the two viruses.

mutants has profound advantages of understanding of many aspects of the viruses, such as viral structure (Drayna and Fields, 1982b), viral assembly (Shing and Coombs, 1996; Hazelton and Coombs, 1999; Becker *et al.*, 2001), viral pathogenesis (Keroack and Fields, 1986; Bodkin and Fields, 1989), and protein function (Drayna and Fields, 1982a; Coombs, 1996). Reovirus temperature sensitivity is classically measured by comparing the ability of the virus to produce plaques when grown on monolayer cells at the nonpermissive and permissive temperatures (Figure 1.4). Dividing the nonpermissive titer by the permissive titer generates an efficiency of plating (EOP) value. Wild-type viruses are expected to have EOP values within an order of magnitude of 1, as they grow equally well at both temperatures. By contrast, *ts* mutants, when examined by the same analysis, will have a value significantly lower than 0.1 (Coombs, 1998).

Our lab has recently generated a set of 17 avian reovirus *ts* mutants by treating wild-type ARV138 with nitrosoguanidine. These *ts* mutants were defined by their reduced capacity to replicate at 39.5 °C (chosen as the non-permissive temperature) as opposed to 33.5°C (chosen as the permissive temperature) (Patrick *et al.*, 2001). A recombination assay is used to determine whether any two of these ARV *ts* mutants have lesions in the same or different genes through pair-wise mixed infections of these *ts* mutants (A×A, B×B, A×B, ... where A and B represent two different *ts* mutant clones). If two *ts* mutants that contain lesions in the same gene segment are crossed, then all progeny viruses will retain this mutation, and the parental *ts* mutants are determined to belong to the same recombination group. By contrast, if two *ts* mutants with lesions in

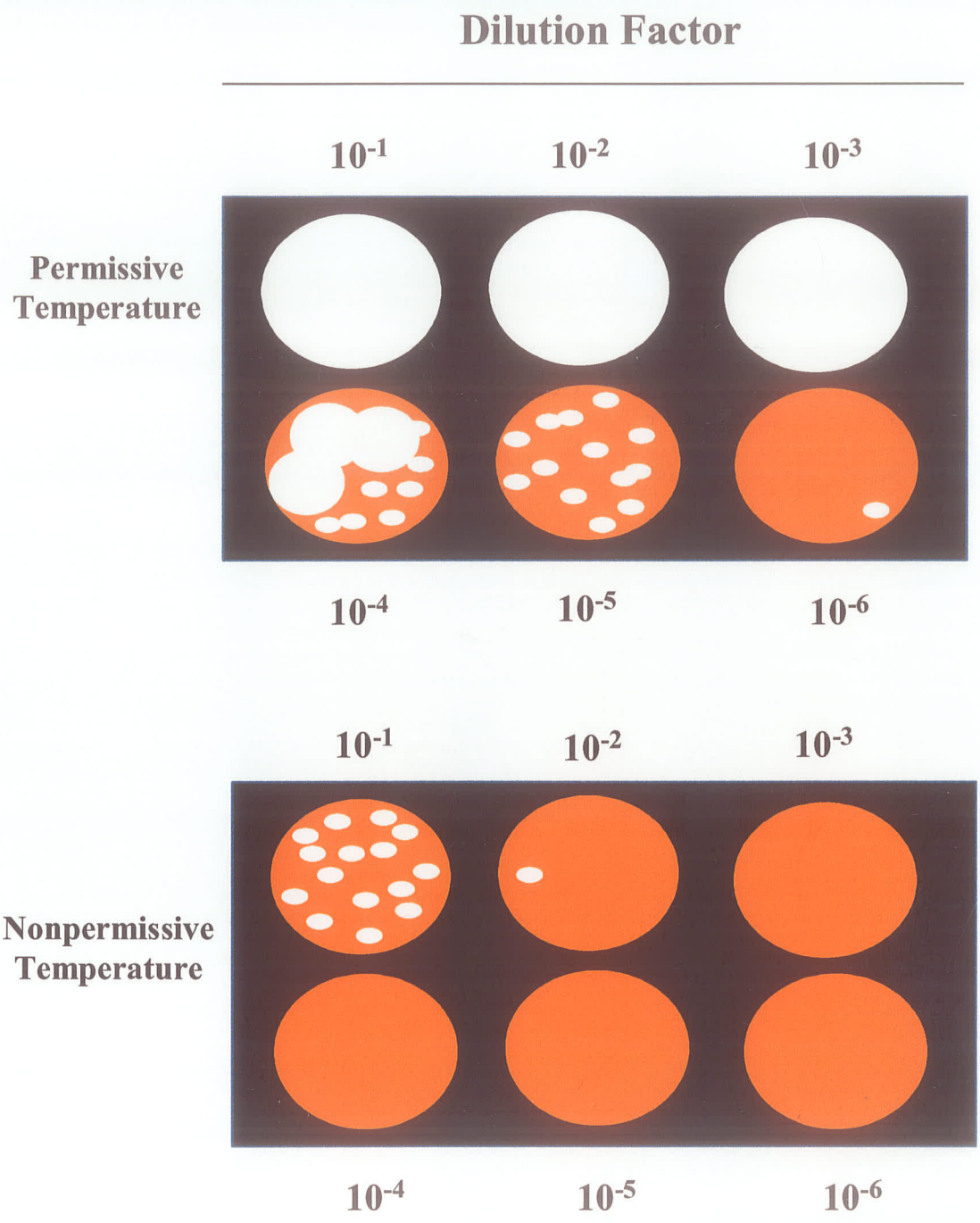
Dilution Factor
10-1
10-2
10-3
Permissive Temperature
10-4
10-5
10-6
10-1
10-2
10-3
Nonpermissive Temperature
10-4
10-5
10-6

Figure 1.4 Cartoon representing the plaque assay for a *ts* clone.

Cell monolayers in 6-well plates were infected with serial 10-fold dilutions of a virus stock and incubated at permissive temperature (e.g. 33.5°C) and nonpermissive temperature (e.g. 39.5°C). Plates were stained with neutral red and plaques (indicated by white dots) were counted to determine the apparent titer at each temperature. The EOP value was determined by dividing the titer at nonpermissive temperature by the titer at permissive temperature. As the *ts* clone is incapable of growing at nonpermissive temperature, its EOP value will be lower than 0.1.

different genes are crossed, some of the progeny viruses will not contain mutated genes and will appear to be wild-type-like. Thus, these two *ts* mutants belong to two different recombination groups. Based on these recombination analyses, 11 of 17 ARV *ts* mutants were assigned to 7 of the 10 expected recombination groups, namely A, B, C...G (Patrick *et al.*, 2001) (Table 1.1). Characterizations of these novel *ts* mutants are limited. Reassortant mapping experiments showed that *tsA12* (one of the two *ts* clones in group A) had its *ts* lesion in the S2 gene, which encodes major core protein σA and *tsD46* (one of the three *ts* clones in group D) had its *ts* lesion in the L2 gene, which encodes RNA dependent RNA polymerase protein, λB (Patrick, 2001). Morphological analysis indicated that defect in *tsA12* leads to an accumulation of cores at nonpermissive temperature. *tsA12* S2 gene has been sequenced and it contains a single alteration of a cytosine to uracil transition at nucleotide position 488, which leads to predicated proline to leucine replacement at amino acid position 158. Paradoxically, many of ARV *ts* mutants fail to produce progeny dsRNA but do synthesize progeny protein at the nonpermissive temperature (Table 1.1).

1.6 Objectives of this research

This research is a continuation of the characterization of avian reovirus *ts* mutants that have been recently generated in our lab (Patrick *et al.*, 2001). Despite the economical importance of ARV, in comparison to MRV, the prototypic member of the genus, less is known about ARV. The use of MRV *ts* mutants has allowed elucidation of many aspects of MRV replication (Zou and Brown, 1996; Roner *et al.*, 1997; Coombs 1998; Keirstead and Coombs 1998; Hazelton and Coombs 1999; Mbisa *et al.*, 2000; Becker, 2001). We have been using assembly-defective MRV *ts* mutants to determine how the multi-

Table 1.1 Genetic groupings and characteristics of avian reovirus temperature-sensitive mutants

Recombination Group	Gene Assignment	Mutant Clone	Nonpermissive (39.5°C) Characteristics		
			dsRNA	Protein	Morphology
A	S2	*ts12*	-	+	Cores
		ts146	-	+	
B		*ts31*	+	++	
C		*ts37*	+	+	
		ts287	+	+	
D	L2	*ts46*	-	+	
		ts195	-	+++	
		ts219	-	+++	
E		*ts158*	-	+++	
F		*ts206*	-	+	
G		*ts247*	-	+	

protein/multi-RNA reoviruses are assembled (Figure 1.5). Precise determination of the molecular mechanisms involved in viral assembly may help to combat disease propagation by targeting susceptible steps along the assembly pathway (Prevelige, 1998). Our knowledge about structure/function and assembly of ARV have lagged behind MRV similar studies, due in part to previous lack of a panel of ARV *ts* mutants to work with. The availability of novel ARV *ts* mutants generated in our lab allows us to continue using this valuable genetic tool with similar studies carried out for MRV.

In this study, *tsA12*, one of group A mutants was reexamined and mutant *tsA146* (another mutant of group A) was examined in parallel. As described in the preceding section, our lab has initially determined that *tsA12* is an assembly-defective mutant, which is not able to assemble past the core. The defect of *tsA12* has been mapped to the S2 gene, which encodes the major core protein σA. The *ts* lesion of *tsA146* may also reside in the S2 gene segment by recombination assay. The temperature sensitivity difference between *tsA12* and *tsA146* has been noted in a past study (Patrick *et al.*, 2001). To determine mutation effect in viral replication, replication capacity of *tsA12* and *tsA146* was examined at different temperatures. *tsA12* appeared more temperature-sensitive than *tsA146*. In the hope of identifying an additional assembly-defective reagent, which could be studied to better understand the role of σA protein in ARV assembly, morphological analysis of *tsA146* was performed in parallel with *tsA12*. *tsA12* was confirmed as an assembly-defective mutant but not *tsA146*. The different phenotypic responses between *tsA12* and *tsA146* are due to different mutations existed in the major core protein σA by sequence analysis.

Characterization of a group B mutant, *tsB31*, was resumed in this research. *tsB31* is a only member of group B. An important step in characterization of a new *ts* mutant is

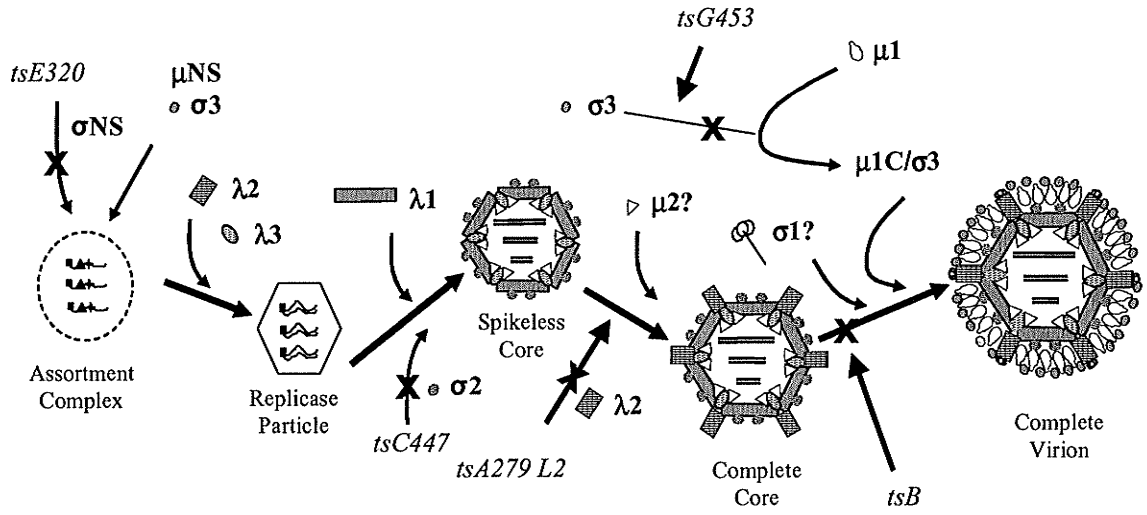

Figure 1.5 Model for mammalian reovirus assembly.

Primary steps in assembly are indicated by thick arrows. Viral proteins participated in each step are indicated. Locations and identities of the eight major structural proteins of the virus are indicated. The blocks in assembly mediated by various *ts* mutants are marked by × at several steps in the pathways.

first to determine the gene segment that harbours the *ts* lesion. Thus, reassortant mapping of *tsB31* was performed. The mutation of *tsB31* was mapped to the M2 gene, which encodes major outer capsid protein μB.

During the course of screening reassortants from mixed infection, some clones appeared to lack a full-length S1 gene segment but were capable of propagation. To understand this phenomenon, some of these clones were investigated. These clones were identified as S1 deletion mutants that had internally deleted S1 gene segments. Sequences that are retained for replication and encapsidation of truncated S1 gene segment were identified to localize at both termini of the S1 genome segment. The first step in viral infection is virus entry into the cells, which is mediated by cell attachment proteins encoded by a virus. For MRV, this cell attachment protein is σ1, which is encoded by S1 gene segment of MRV and a minimum of three σ1 trimers per particle was required for full infectivity (Larson *et al.*, 1994). The cell attachment protein of ARV is σC, which is also encoded by its S1 genome segment. The gene that encodes this protein was severely impaired in the S1 deletion mutants and therefore is not expected to have any functional cell attachment proteins to be synthesized. Paradoxically, these S1 deletion mutants were capable of replicating to relatively higher titers at the permissive temperatures when compared to its wild-type parent, ARV 138. This suggests that some mechanisms involved in ARV entry into cells may differ from its counterpart MRV.

Taken together, evidence shown in this research programme highlights the need to explore the poorly understood avian reoviruses.

CHAPTER 2 MATERIALS AND METHODS

2.1 Stock viruses and cells

Avian reovirus strains 138 (ARV138) and 176 (ARV176) are laboratory stocks. Temperature sensitive (*ts*) mutant clones *tsA12* and *tsB31* [originally derived from ARV138 as described (Patrick *et al.*, 2001)], and reassortant clones derived from ARV176 × *tsA12* cross that were generated by Megan Patrick are laboratory stocks. All viruses were grown in the QM5 continuous quail fibroblast cell line. The cells were maintained in 1× Medium199 supplemented with 10% fetal calf serum (Gibco BRL), 10% tryptose phosphate broth (2% tryptone, 0.2% dextrose, 8.6 mM NaCl, 1.8 mM Na_2HPO_4), and 2 mM l-glutamine and grown in the presence of 5% CO_2 at 37°C. Confluent cell monolayers were routinely split (1:6) twice weekly by standard trypsinization procedures. Viral infections were carried out on cell monolayers supplemented with 100 U/ml of penicillin, 100 µg/ml streptomycin sulfate, and 1 µg/ml amphotericin-B as described (Coombs *et al.*, 1994).

2.2 Viral manipulation

2.2.1 Virus passaging

Wild-type viruses, *ts* mutants and reassortant virus stocks were amplified in QM5 cells grown in supplemented Medium 199 (as described above). Once QM5 cell monolayers reached 90% confluency, growth media was then removed (some saved as "pre-adaptive" media) and the cells were subsequently infected with stock virus at a multiplicity of infection (MOI) less than 1 plaque forming unit (PFU) per cell. Virus was

allowed to adsorb to the cell monolayer for 1 hour at room temperature with periodic mixing every 10 to 12 minutes. After adsorption, fresh supplemented Medium 199 containing 25% pre-adapted medium was then added and the infected monolayers were incubated at 37°C for wild-type clones and at 33.5°C for *ts* and reassortant clones. Cells were examined daily with the light microscope to check for cytopathic effect (CPE). Once the monolayers displayed ~ 90% CPE, infected cells were harvested and disrupted by three cycles of freeze-thawing at -80°C. Viruses were titered by plaque assay as described below and stored at 4°C for immediate use.

2.2.2 Virus Plaque Assay

Serial 1:10 dilutions of virus were made in gel saline (137 mM NaCl, 0.2 mM $CaCl_2$, 0.8 mM $MgCl_2$, 19 mM HBO_3, 0.1 mM $Na_2B_4O_7$, 0.3% [wt/vol] gelatin). Sub-confluent QM5 cell monolayers in 6-well tissue culture plates were infected by a volume of 100 µl of each dilution after removal of growth media. The virus was allowed to adsorb for one hour with periodic mixing every 10 to 12 minutes. After adsorption, each well was overlayed with 3 ml of a 1:1 ratio of 2% agar and 2 × Medium 199 supplemented with 10% FCS and a final concentration of 2 mM l-glutamine, 100 U/ml of penicillin, 100 µg/ml streptomycin sulfate, and 1 µg/ml amphotericin-B. The cells were fed with 2 ml fresh agar/199 (supplemented as above) at 3 days post infection (dpi) for cells grown at 37 or 39.5°C, at 4 dpi for cells grown at 33.5°C. Cells were then stained with a 0.02% neutral red solution [neutral red in a 1:1 ratio of 2× phosphate buffered saline (PBS) to 2% agar] at 4 dpi for cells grown at 37 or 39.5°C, at 6 dpi for cells grown at 33.5°C. Viral plaques were counted 18 hours after they were stained and the viral titres were calculated.

2.2.3 Virus purification

Sub-confluent QM5 cells in P150 tissue culture dishes were infected with viral clones at an MOI of 5 PFU/cell. After viral adsorption for 1 hour at room temperature, cell monolayers were overlaid with Medium 199 supplemented as described in 2.2.1. Viral infections were carried out at 37°C for wild-type viruses and at 33.5°C for *ts* mutants. When ~ 60% CPE was displayed, cells in P150 dishes were scrapped into the culture medium. Cells were pelleted at 3,500 rpm for 20 minutes in a fixed-angle rotor (JA-10) in a Beckman RC centrifuge (Beckman, Mississauga, ON). The cells were resuspended in HO buffer (10mM Tris-HCl, pH 7.4, 250 mM NaCl, 10 mM β-mercaptoethanol) and transferred to a 30-ml COREX tube. Cells were disrupted by sonication for 10 seconds. Cell membranes were further disrupted with the addition of 1/50 sample volume of 10% DOC (desoxycholate) followed by vortexing and incubation on ice for 30 minutes. Virus was extracted with Vertrel XF (1,1,1,2,3,4,4,5,5,5-decafluoropentane) (DuPont Chemicals, Wilmington, DW), and purified in 1.2-1.45 g/cc cesium chloride gradients as previously described (Mendez *et al.*, 2000). Virus bands were harvested and dialyzed extensively against D-Buffer (Dialysis Buffer, 150 mM NaCl, 15 mM $MgCl_2$, 10 mM Tris, pH 7.4) to remove cesium chloride. Virus was collected into appropriate vessels and stored at 4°C or frozen with the addition of 25% glycerol at -80°C.

2.3 Virus growth curves

The abilities of various ARV clones to replicate at various temperatures were determined by infecting QM5 cells in 24-well culture dishes at an MOI of 10 PFU/cell for

1 hour at room temperature. After adsorption, the inoculum was removed, and the monolayers were washed with 1 × PBS twice and overlaid with Medium 199. At various times post infection, the cells were harvested and disrupted by freeze thawing twice and sonication. The yield of infectious progeny virions was determined by plaque assay on QM5 cells as described in 2.2.2.

2.4 Determination of temperature sensitivity

An efficiency of plating (EOP) assay was used to determine whether a virus clone was *ts*. Sub-confluent 6-well tissue culture plates were infected with serial 1:10 dilutions of a virus stock in duplicate, incubated, and stained with neutral red at 33.5°C (permissive temperature) and 39.5°C (non-permissive temperature) as described in section 2.2.2. The viral titre was determined by plaque counts obtained at each temperature. EOP values for each virus were determined by dividing the nonpermissive titer by the permissive titer. EOP values near 1.0 were considered to indicate the non-*ts* phenotype, while EOP values at least 10-fold lower than that of wild-type were considered to indicate *ts* phenotype (Coombs, 1998).

2.5 Reassortant mapping

2.5.1 Generation of reassortants

A sub-confluent QM5 cell monolayer in one well of a 24-well tissue culture plate was co-infected with ARV176 and *tsB31*, each at an MOI of 10 plaque forming units. After 1 hour adsorption at room temperature, the viral inoculum was removed and the cell monolayer was overlaid with 500 µl completed medium 199 supplemented with 1 × penicillin-streptomycin sulfate, and 1 × amphotericin B, and incubated at 33.5°C for 32

hours. The infection was freeze/thawed twice, and sonicated for 10 seconds to lyse the cells. Three serial 1:100 dilutions of the mixed infection were made in gel saline, followed by 3 serial 1:3 dilutions. Each of the final 3 dilutions was used to infect 5 P100 tissue culture dishes with 300 µl of virus. After adsorption, the viral inoculum was removed and the cells were overlaid with 15 ml of a 1:1 ratio of 2% agar and 2 × Medium 199 and incubated at 33.5°C for 9 days. The infections were fed with 12 ml of a 1:1 ratio of 2% agar and 2 × Medium 199 on day 5. The plates were stained with 12 ml 0.02% neutral red on day 9. Plaques separated from each other by more than 0.75 cm were picked and placed in 2-dram vials with 0.5 ml completed medium 199 supplemented with 2× penicillin-streptomycin sulfate and 2× amphotericin B overnight at 4°C to allow viruses to diffuse out of the agar plug (P_0). 350 µl Medium 199 (supplemented as above) containing QM5 cells at 4.2×10^5 cells/ml were added to each of the vials. The vials were incubated at 33.5°C for 9 days and then freeze/thawed 3 times at -80°C to generate P_1 viral stocks. The P_1 stocks were subsequently amplified in T25 flasks at 33.5°C as described earlier to generate P_2 viral stocks.

2.5.2 Isolation of viral genome

P100 tissue culture dishes with subconfluent QM5 cell monolayers were infected with 350 µl of P_2 progeny clones and incubated at 33.5°C until ~75% CPE was observed. Cells were harvested by scraping the cell monolayers and transferred to centrifuge tubes. Cells were then pelleted at 1100 rpm for 10 minutes in the IEC floor centrifuge. The cell pellets were resuspended in 500 µl of NP-40 buffer containing140 mM NaCl, 1.5 mM $MgCl_2$, 10mM Tris, pH 7.4, and 0.5% NP-40 detergent, incubated on ice for 30 minutes

with periodic vortexing every 10 minutes. Cellular nuclei and organelles were pelleted at 1100 rpm in the IEC floor centrifuge and supernatants were transferred to sterile microfuge tubes (Fisher, Nepean, ON). A mixture of 30 µl of 1 M Tris, pH 7.8, 3 µl of 200 mM EDTA, pH 8, 60 µl of 10% SDS was added to each sample. Samples were then heated for 15 minutes at 42°C and the viral dsRNA genomes were extracted once with 600 µl of phenol/chloroform (1:1). Samples were vortexed and then reheated at 42°C for 30 seconds followed by centrifugation at 12,500 rpm for 5 minutes. The top aqueous phase was transferred to a sterile microcentrifuge tube and placed on ice. Viral dsRNA was precipitated with 1/10th volume of sodium acetate (3M, pH 5.2) and 2.5 volumes of ice-cold absolute ethanol at -20°C overnight, and then pelleted at 12,500 rpm for 30 minutes at 4°C in the Biofuge microcentrifuge (VWR Scientific, Toronto, ON). The viral RNA pellet was vacuum dried (SC100 speed-vac, Savant, Holbrook, NY), then resuspended in 30 µl of 1× electrophoresis sample buffer (240 mM Tris-HCl, pH 6.8, 1.5% dithiothreitol, 1% SDS).

2.5.3 Identification of reassortants by sodium dodecyl sulfate polyacrylamide gel electrophoresis (SDS-PAGE)

12.5% polyacrylamide slab gels (16 cm × 16 cm × 0.1 cm) were poured and polymerized overnight. RNA samples prepared (as described in section 2.5.2) were heated at 65°C for 5 minutes and then electrophoresed at 18 mAmps/gel for 1.5 hours, 12 mAmps/gel for 66-70 hours, and 2 mAmps/gel for 3-5 hours. Viral genome segments were stained with ethidium bromide, and photographed under UV irradiation.

Reassortants were identified by comparing the migration patterns of the progeny RNA gene segments to those of the parents involved in co-infection.

2.6 Electron microscopy of negative stained ARV particles

Subconfluent QM5 monolayers in 24-well tissue culture dishes were infected in duplicate with ARV138, *tsA12*, or *tsA146* at an MOI of 10 PFU/cell. After attachment for 1 hour at 4°C, the inoculum was removed, and the monolayers were washed with 1 × PBS twice. The infections were overlaid with 500 µl of completed Medium 199, and incubated for either 22 hours at 39.5°C or 30 hours at 33.5°C (approximately one round of replication). Infections were freeze/thawed three times, and the cell debris was cleared by centrifugation for 3 minutes at 15,000 rpm in an Eppendorf Model 5412 centrifuge. Then, 50-µl aliquots of the supernatants were centrifuged for 1 hour over 100-µl cushions of 30% potassium tartrate (pH7.2) in the Airfuge® (Beckman Instruments, Palo Alto, C; A100 rotor) at 26 psi to obtain viral and subviral pellets. Pellets were resuspended in 1× Medium199 supplemented with 0.1% glutaraldehyde, allowed to fix for 10 minutes on ice, centrifuged directly onto Formvar-coated, carbon-stabilized 400-mesh copper electron microscopy grids for 30 minutes at 26 psi (Airfuge®, EM-90 rotor). The samples were stained with 2.5 mM phosphotungstic acid and viewed at magnifications between 30,000× and 70,000× in a Philips 201 EM operated at an acceleration voltage of 60 Kev. The relative proportions and types of particles produced in each infection were determined by direct counting of all particles in each of five non-adjacent grid squares from the four outer quadrants and the central area of the grid.

2.7 Sequencing the *tsA146* S2 gene

2.7.1 Viral RNA extraction

QM5 cells were infected with *tsA146* at an MOI of 10 PFU/cell and incubated at 33.5°C until appearance of 90% CPE. Cells were freeze/thawed three times and cell debris was removed by centrifugation at 13,500 rpm for 5 minutes. 200 µl of clarified culture lysate was added to a 1.5-ml microcentrifuge tube containing 11.75 µl of 1 M Tris (pH 8.0), 2 µl of 200 mM EDTA (pH 8.0), and 23.5 µl of 10% SDS, and the tube was incubated at 42°C for 15 min. The genomic dsRNA was extracted twice with phenol-chloroform and once with chloroform. dsRNA was precipitated overnight at -20°C with 1/10th volume of sodium acetate and 2.5 volumes of ice-cold absolute ethanol and washed with 70% ethanol. The dsRNA pellet was then resuspended in 6 µl of 90% DMSO (dimethyl sulfoxide) and 10% 10mM Tris-HCl, pH 6.8.

2.7.2 Primers

The two end primers and five internal primers (Table 2.1) that were used for ARV S2 gene amplification (primer ARV # 1 and primer ARV # 5) and sequencing (primers ARV # 1, # 2, # 3, # 5, # 6, # 7, and # 8) were designed from ARV 138 S2 gene sequence (GeneBank accession # AF059717) by a former student in the lab, Megan Patrick.

2.7.3 Reverse transcription and PCR amplification

The purified viral dsRNA (6 µl) was added to a 0.6-ml microcentrifuge tube containing 1 µl of 2 µM gene-specific primer (ARV # 1 or ARV # 5), 1 µl of 10 mM dNTP mixture (10 mM each of dATP, dGTP, dCTP, and dTTP), 4 µl DEPC (diethylpyrocarbonate)-treated ddH_2O (double distilled water). The mixture was heated at

Table 2.1 Oligonucleotide primers for RT-PCR amplification and sequencing of ARV S2 gene

Primer	Polarity	Nucleotide position	Sequence (5' → 3')
ARV # 1	+	1-18	GCTTTTTCTCCCACGATG
ARV # 2	+	421-444	CGTGAGCTGCAATCTAAATACCCG
ARV # 3	+	904-923	CGTCAACCGCCGATGTTTGC
ARV # 5	-	1303-1288	CCGGAGGGCTGGACTC
ARV # 6	-	1029-1006	GATGCATTCCTGCGCGGTAGTTAG
ARV # 7	-	583-559	CGCACATGTCAACGAAATTGTTACC
ARV # 8	-	204-181	CAACGAACCTGGATAGGGTGCTTC

94°C for 5 min and quick chilled on ice. After the addition of 4 µl of 5 × First-Strand Buffer (250 mM Tris-HCl, pH 8.3, 375 mM KCl, 15 mM $MgCl_2$), 2 µl of 0.1 M DTT (dithiothreitol), 1 µl of RNaseOUT™ Recombinant Ribonuclease Inhibitor (40 units/µl), and 1 µl (200 units) of SuperScript™ II reverse transcriptase (Invitrogen). The mixture was incubated at 42°C for 1.5 hours.

The cDNA produced by reverse transcription was amplified using the Expand™ Long Template PCR System according to the manufacturer's instructions (Roche). Polymerase chain reaction (PCR) was performed in 50-µl volumes containing 5 µl of 10 × Expand™ Long Template PCR Buffer 3, 1 µl of 10 mM dNTP mixture, 1 µl of 10 µM upstream primer (ARV # 1), 1 µl of 10 µM downstream primer (ARV # 5), 0.75 µl of Expand™ Long Template enzyme mixture (5 U/µl), 2 µl of cDNA, and 39.25 µl of autoclaved ddH_2O. The amplification reaction was carried out in a GeneAmp PCR System 9700 thermal cycler (Applied Biosystems) with (i) preliminary denaturation for 3 min at 94°C, followed by (ii) 35 cycles of denaturation at 94°C for 1 min, annealing at 55°C for 1 min, and primer extension at 68°C for 2 min and (iii) a final product extension at 68°C for 7 min. The amplification product was visualized by ethidium bromide staining and UV transillumination following electrophoresis on a 1% agarose gel in 0.5× TBE buffer (4.5 mM tris, 4.5 mM boric acid, and 0.9 µM EDTA). A gel electrophoresis band of about 1300 bases was considered to be the product of a specific amplification of the targeted ARV S2 gene and then excised from the gel using a sterile razor blade on top of a UV light box and purified by QIAquick™ gel extraction kit (Qiagen, Germany) according to the manufacturer's instructions.

2.7.4 Cycle sequencing

Cycle sequencing was carried out by using the ABI PRISM® BigDye™ Terminator Cycle Sequencing Ready Reaction Kit (Perkin Elmer {PE} Applied Biosystems, Foster City, CA). The nucleotide sequence of *tsA146* S2 gene was determined in both directions. Each sequencing reaction was set up to contain 3.2 pmol of primer, 30-90 ng of cDNA template, 2 µl BigDye™ Terminator Ready Reaction Mix (consisting of dye terminators, dNTP's, r*Tth* pyrophosphatase, $MgCl_2$, Tris-HCl buffer, pH 9.0, and the AmpliTaq DNA Polymerase, FS), and deionized water to a final volume of 5 µl. Cycle sequencing was performed on a GeneAmp PCR system 9700 for 1 cycle of 96°C for 3 minutes, followed by 40 cycles of 96°C for 30 seconds, 52°C for 30 seconds, and 60°C for 4 minutes. The products were precipitated with 1/10th volume of sodium acetate (3M, pH 4.6) and 2.5 volumes of ice-cold absolute ethanol at room temperature between 15 minutes to 24 hours, washed, dried, and resuspended in 20 µl formamide. The sample was then heated at 95°C for two minutes and immediately followed by snap cooling in ice-water. The ABI PRISM 3100 Genetic Analyzer (PE Applied Biosystems Foster City, CA) was used to determine the sequence for each reaction. Chromas version 2.13 (McCarthy, 2001) was used to manually analyze sequences to ensure accuracy. Assembly of the nucleotide sequence data was performed using Sequencher™ 3.1.1 software (company). MegAlign (DNASTAR Inc., Madison, WI) was used for sequence comparison between ARV 138 and *tsA146*.

2.8 Placement of σA mutation within reovirus core crystal structure

The position of avian reovirus σA mutation relative to that of MRV σ2 was identified by amino acid sequence alignments using MegAlign in DNASTAR (DNASTAR, Inc., Madison, Wis.). The mammalian reovirus core crystal structure (PDB # 1EJ6) (Reinisch *et al.*, 2000) was manipulated with PyMOL (DeLano, 2003) to identify probable locations of ARV σA and MRV σ2 mutations.

2.9 Restriction endonuclease digestion

2.9.1 RT-PCR amplification of the M2 gene segment

Genomic dsRNA of ARV 176, *tsB31*, or reassortant clone 231 (generated from ARV 176 × *tsB31*) was prepared as described in section 2.7.1. An upstream primer (5'-GCTTTTTCAGTGCCAGTCTTT-3') and a downstream primer (5'- ATGAATAACGTG CCAATCCA-3') were designed from alignments of ARV 138 and ARV 176 M2 gene sequences kindly provided by Dr. R. Duncan (Dalhousie University, Halifax, Canada; unpublished data). The primers were ordered in a desalted form from Invitrogen (Life Technologies), resuspended in DEPC-treated water and their concentration determined by UV spectroscopy. RT-PCR was performed as described in section 2.7.3 with cycle reaction programme changed as the following: preliminary denaturation for 3 min at 94°C, followed by 35 cycles of denaturation at 94°C for 1 min, annealing at 52°C for 1 min, and primer extension at 68°C for 2 min 30 sec, and a final product extension at 68°C for 7 min. Reaction products were analyzed by electrophoresis on a 0.8% agarose gel and products corresponding to ~ 2150 bases were excised and purified using QIAquick™ gel extraction kit (Qiagen, Canada).

2.9.2 Restriction enzyme analysis

The DNA product obtained by RT-PCR was quantified and 5 µl of the DNA solution containing 0.2-1 µg of DNA was digested by either 1 µl of *Eco*RV (10 U/µl; Promega) or 1 µl of *Sac*II (10 U/µl; Promega), adjusted to a final volume of 20 µl with 2 µl of the corresponding buffer and 12 µl of ddH_2O. The digestions were incubated for 1.5 hr at 37°C. DNA fragments were resolved by migration in a 2% agarose gel containing 1 µg/ml ethidium bromide, and the gel was examined under UV light.

2.10 Determination of the nucleotide sequence of the truncated S1 genome segment

2.10.1 RT-PCR amplification of the S1 genome segment

Virus template was obtained from purified ARV 138, ARV 176, or S1 deletion mutant virions. The genomic dsRNA was extracted, precipitated, and resuspended as described in section 2.7.1.

The S1 segment nucleotide sequence of the ARV 138 is available on GenBank (Accession # AF218359) and was used to design terminal primers (Figure 2.1). The forward oligonucleotide primer, GCTTTTTCAATCCCTTGTTTGTC, corresponds to the 5' plus-sense end of the genome segment and the reverse oligonucleotide prime, GATGAATAACCAATCCCCGTAC, corresponds to the 5' reverse sense end of the genome segment. RT-PCR was performed using methodology described in section 2.7.3, but with the following changes: cycle reaction was performed with preliminary denaturation for 5 min at 94°C, followed by 30 cycles of denaturation at 94°C for 1 min, annealing at 55°C for 1 min 30 sec, and primer extension at 70°C for 2 min, and a final product extension at 70°C for 7 min. The reaction product was electrophoresed on a 1.5%


```
   1 5'gctttttcaa tcccttgttt gtcgatgctg cgtatgcctc ccggttcgtg taacggtgca
  61   acagctatct ttggtaacgt ccattgtcag gcggctcaaa atactgccgg cggcgacttg
 121   caagctacct catccataat tgcctattgg ccttatctag cggcgggtgg tggtttttg
 181   ttgattatta ttatttttgc catcttctac tgttgtaagg ctaaagttaa agcggacgct
 241   gcacggagtg ttttccaccg tgagcttgta gcactgagct ctggtaagca caatgcaatg
 301   gctccgccat acgacgtttg aagtgcaacg ctttgatttc tgcccaatat cacttcgtga
 361   gcttgccacc ccatcgttta ctgctataat tgggattgac ccatcacgtt attttaatat
 421   tgagctttcg cacacgcatc ctctctactc taagttgccg actctgttat cgcagccctg
 481   ccgagtccac gtgcgtttga ttcgtagatt cgctctctgt tcaacgctgt cgagtatctg
 541   cgagtacgat tgtgcgttac tactttcccc acacgccatc actccactgt cctcatccga
 601   tcagcgatct tatcttatag ttcattggga tggcgggtct caatccatca cagcgaagag
 661   aggtcgtcag cttgatactg tcattgactt cgaacgcgca tataaatcat ggcgatttga
 721   cgccaatcta tgaacggttg accagtttag aagcgtctgc ggaatcacta tatcgctcca
 781   tttccagcat gtctactacc gtttcagaca tttcagcaga tttgcagaac gtgactcgcg
 841   ccttggatga tgtgactgct aatttagatg gtatgagagt caccattact acgcttcaag
 901   attctgtgtc cactctctca acgactgtaa ctgatttaac aaacacctct tctgtgcact
 961   cggaagcact gtcttcactc cgaactatag ttgatgggaa ctccactacc attgataatt
1021   tgaaaagtga tgtatcatca aacggtcttg ctatcacaga cctgcagagt cgtgttaaat
1081   ccttggaatc tgtttcgagt cacgggctat ctttttcgcc tcctcttagt gtcgctgacg
1141   acgtagtgtc gttgagtatg gacccttact tttgctctca gcgagtcacc ttgacatcat
1201   actcagcaga agctcaactg atgcaattcc aatggatggc aagaggtgct aacggatcat
1261   cagacactat tgacatgacc gtcaatgctc actgtcatgg gagacgcact gattacataa
1321   tgtcgtccac gggaggtctt acagttacta gtaatgccgt gtctttaacc ttcgacttga
1381   gttacattac acgcctccca ccagacctct cgcgtcttgt tcccagtgca ggattccaag
1441   ccgcgtcgtt ccccgtggat gtatccttca ccagagattc gacaactcat acatatcaag
1501   cttatggagt gtattctagt tcgcgtgtat ttaccatcac tttcccgact ggtggtgacg
1561   gtcccgcaaa tatccgtttc ctaaccgtgc gtaccggcat cgacacctaa ggtgtggcgc
1621   cgtacgggga ttggttattc atc 3'
```

Figure 2.1 ARV 138 S1 segment sequence and the location of terminal primers.

The nucleotide sequence of ARV 138 S1 genome segment was obtained from GeneBank (Accession number AF218359). The plus strand of the genome segment is shown 5' to 3'. Green arrow indicates where forward primer binds to the 3' end of minus strand. Blue arrow indicates where reverse primer binds to the 3' end of plus strand.

agarose gel. The resultant band with expected size was excised and the dsDNA was then extracted from the agarose using the QIAquick™ gel extraction kit (Qiagen, Canada).

2.10.2 Cycle sequencing

Sequences of the eluted cDNAs obtained from section 2.10.1 were determined in both directions by using same primers described in section 2.10.1. Cycle sequencing was carried out in 5-µl volumes using the ABI PRISM® BigDye™ Terminator Cycle Sequencing Ready Reaction Kit (Perkin Elmer {PE} Applied Biosystems, Foster City, CA) as described in section 2.7.4. Nucleotide sequence data was analyzed with DNASTAR (DNASTAR, Inc., Madison, Wis.).

2.11 Statistical analysis

The nonparametric Mann-Whitney sum test was used to determine the relative contribution of any single gene in reassortant mapping experiments. The chi-square test was used to determine significance of morphological changes examined by electron microscopy. The p value was calculated using programme provided by GraphPad Software, Inc. (WWW.graphpad.com).

CHAPTER 3 RESULTS

3.1 Characterization of *tsA12* and *tsA146*

As mentioned in the introduction, avian reovirus *ts* mutants have been assigned to 7 recombination groups. Group A contains two clones, *tsA12* and *tsA146*. *tsA12* was the prototypical mutant in group A. Reassortant mapping experiments showed that this mutant had its *ts* lesion in the S2 gene, which encodes major core protein σA. Initial morphological analysis of this mutant indicated an accumulation of core particles at non-permissive temperature. This phenotypic response is due to a single amino acid change of proline to leucine at amino acid position 158 in σA protein. Furthermore, *tsA12* was found to be incapable of synthesizing dsRNA but does produce decreased amounts of protein at nonpermissive temperature.

To gain more understanding of *tsA12*, its *ts* properties were further characterized and compared with the other mutant in the same group, *tsA146*. To confirm *tsA12 ts* phenotype seen at restrictive temperature, particle counting of infected cell lysates was also performed. Localization of *ts* lesion in *tsA12* was confirmed by reassortant mapping.

3.1.1 Comparison of replicative abilities of *tsA12*, *tsA146*, and ARV 138

The previous efficiency of plating assay indicated that clone *tsA12* exhibits temperature sensitivity at temperature of 37°C whereas *tsA146* displays the *ts* phenotype at temperatures in excess of 38°C (Patrick *et al.*, 2001). To determine the rate and extent of impaired replication of these two viruses at elevated temperatures, QM5 cell monolayers were infected with *tsA12*, *tsA146*, or ARV 138 and incubated at various temperatures from 33.5 to 39.5°C, and infections were harvested at desired times of post-infection and the titers of infectious progeny virions were determined by plaque assay.

There was little difference between the infectious progeny virus production of *tsA12* and its parental wild-type ARV 138 at temperature of 33.5°C (Figure 3.1A). The final yield from cultures infected with *tsA146* was reproducibly 2- to 7-fold higher than corresponding cultures infected with ARV 138 and *tsA12* at 33.5°C after the 12 hour viral eclipse phase (Figure 3.1A). At increased temperatures of 37 to 39.5°C, in contrast to the replication of ARV 138 that was only marginally changed, the titers of *tsA12* were 50- to 80-fold lower than those of wild-type ARV 138 at various times postinfection (p.i.) after the 6 hour viral eclipse phase (Figure 3.1B-E). At 37°C and 38°C, the titers of *tsA146* were reduced 4- to 8-fold relative to titers obtained after ARV 138 infection, respectively (Figure 3.1B-C). At higher temperatures of 39°C and 39.5°C, the titers of *tsA146* were dramatically decreased 30- to 40-fold compared to titers obtained from ARV 138, respectively (Figure 3.1D-E). While the replication of *tsA12* was severely impaired starting at 37°C (Figure 3.1F), the replication of *tsA146* was progressively reduced along with increased temperatures (Figure 3.1F).

3.1.2 Morphological analysis of *tsA12* and *tsA146*

A general first step in characterizing the nature of the defect in a *ts* mutant is to determine the morphological effect of the mutation. This has been done for many of the MRV mutants by electron microscopy (Fields *et al.*, 1971; Danis *et al.*, 1992; Coombs *et al.*, 1994; Hazelton and Coombs, 1995). With ARV, this type of study has recently been initiated. To confirm previous observation that *tsA12* assembles core particles at nonpermissive temperature and also to assess if *tsA146*, whose *ts* lesion(s) is predicted to localize in the same gene with *tsA12* by recombination assay, has similar phenotypic

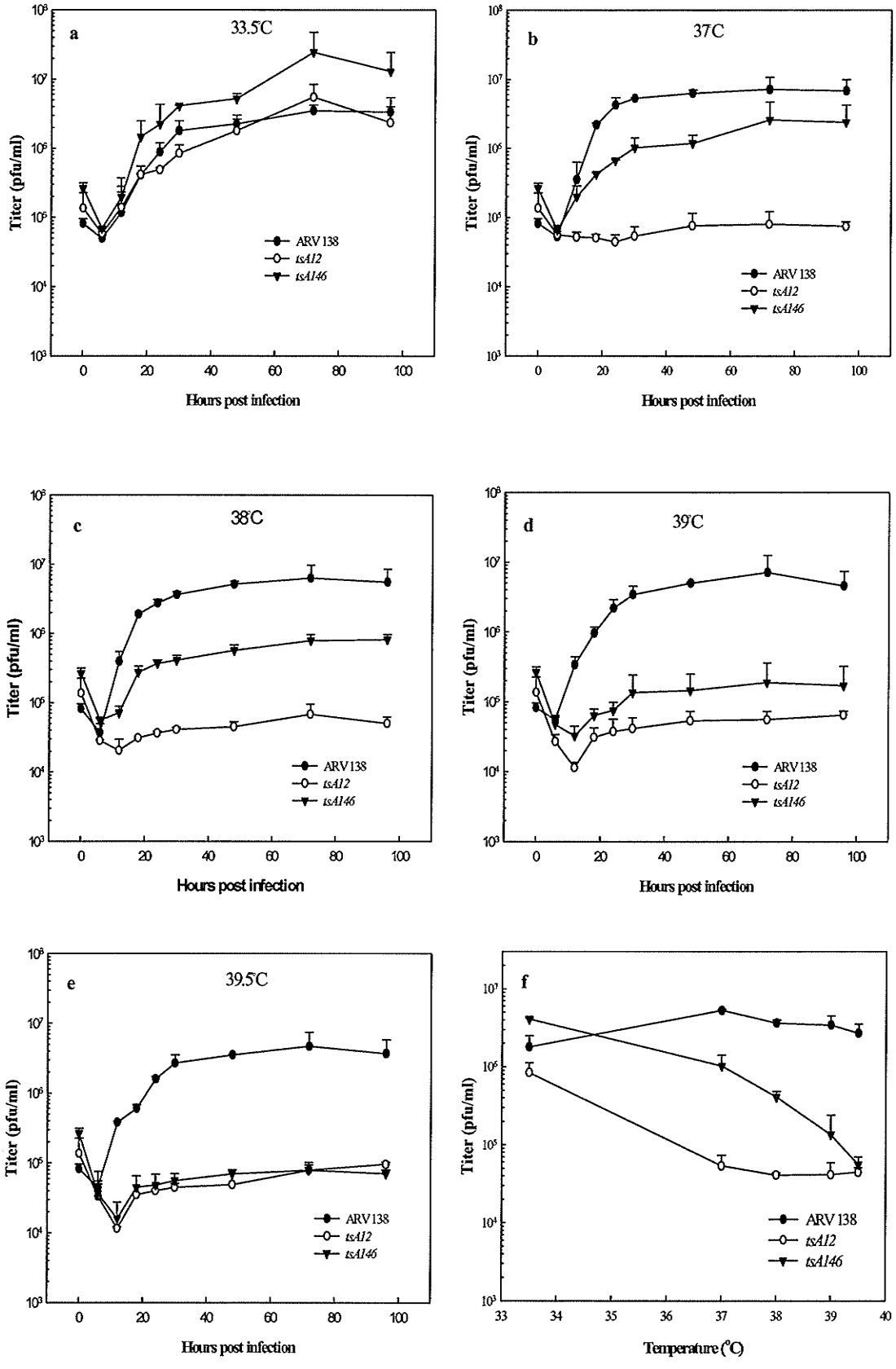
a
33.5°C
b
37°C
c
38°C
d
39°C
e
39.5°C
f
Titer (pfu/ml)
Hours post infection
Temperature (°C)
ARV138
tsA12
tsA146

Figure 3.1 Kinetics of viral growth in QM5 cells at various temperatures.

QM5 cell monolayers were infected with ARV 138, *tsA12*, or *tsA146* at an MOI of 10 PFU/cell and incubated at 33.5°C (A), 37°C (B), 38°C (C), 39°C (D), and 39.5°C (E). At various times postinfection, the monolayers were harvested, and the yield of infectious progeny virions was determined by plaque assay. Results are the average of two separate experiments and the error bars represent one standard deviation. The replicative abilities of individual virus at 30 h.p.i. at various temperatures compiled from A, B, C, D, and E are shown in F.

response with *tsA12* at nonpermissive temperature, morphological analysis of *tsA12* and *tsA146* were performed.

QM5 cells infected with *tsA12*, *tsA146* or parental wild-type ARV138 at both permissive (33.5°C) and restrictive temperatures (39.5°C) were processed and examined by electron microscopy as described in Materials and Methods. Direct particle counting of all types of particles released from lysed cells was carried out and compared to types of particles produced by ARV138. Table 3.1 and Figure 3.2 show the average proportions of structures produced by ARV138, *tsA12*, and *tsA146* at both permissive and nonpermissive temperatures from two to three separate experiments. The predominant structural forms produced by ARV138 at both permissive and restrictive temperatures were complete virion and top component (Table 3.1). Proportions of all particles produced by ARV138 were similar at both temperatures. Cells infected with ARV 138 at the permissive temperature produced approximately 3 times as much virus and sub-viral particles as cells infected with ARV 138 at the nonpermissive temperature. *ts* mutants grown at nonpermissive temperature produced fewer viral particles than those grown at permissive temperature (approximately 100-fold decline for *tsA12* and 80-fold decline for *tsA146*). Cells infected with *tsA12* and grown at the nonpermissive temperatures produced approximately 80-fold fewer viral particles than cells infected with ARV 138 and grown at then nonpermissive temperature. Cells infected with *tsA146* produced 13-fold fewer viral particles at 39.5°C compared to cells infected with ARV 138 at 39.5°C. The distribution of particles produced by the mutants was different from the distribution of ARV 138 particles. At 33.5°C, the most common type of particle produced by *tsA12*

Table 3.1 Distribution of types of particles produced by ARV138 and *tsA12* at permissive and nonpermissive temperatures[a]

Clone	Temp(°C)	Total no. of particles[b]	Total no. of particles/ml[c]	Proportion of particle(% [SEM])[d]			
				Viron	Top component	Core	Outer shell
ARV138	33.5	5273	2.2×10^9	40.4 (7.7)	53.0 (6.0)	3.7 (1.8)	2.9 (0.4)
	39.5	28127	7.2×10^8	43.7 (15.7)	50.7 (15.5)	2.9 (0.7)	2.7 (0.2)
tsA12	33.5	1524	8.9×10^8	69.8 (21.2)	18.7 (19.1)	5.0 (2.6)	6.5 (1.1)
	39.5	783	9.6×10^6	24.8 (7.5)	35.0 (8.9)	31.1 (18.6)	9.1 (2.5)
tsA146	33.5	6923	4.2×10^9	37.8 (9.1)	50.8 (8.6)	6.4 (0.5)	5.0 (0.9)
	39.5	3185	5.6×10^7	62.8 (14.9)	33.1 (11.38)	2.1 (4.6)	2.0 (1.0)

[a] Calculated from three separate experiments.

[b] Total number of viral and subviral particles counted.

[c] Total number of particles in the cell lysates, calculated as previously described (Hammond et al., 1981).

[d] Proportion of indicated particle type, expressed as the percentage of the total number of particles produced, with standard error of the mean shown in parentheses.

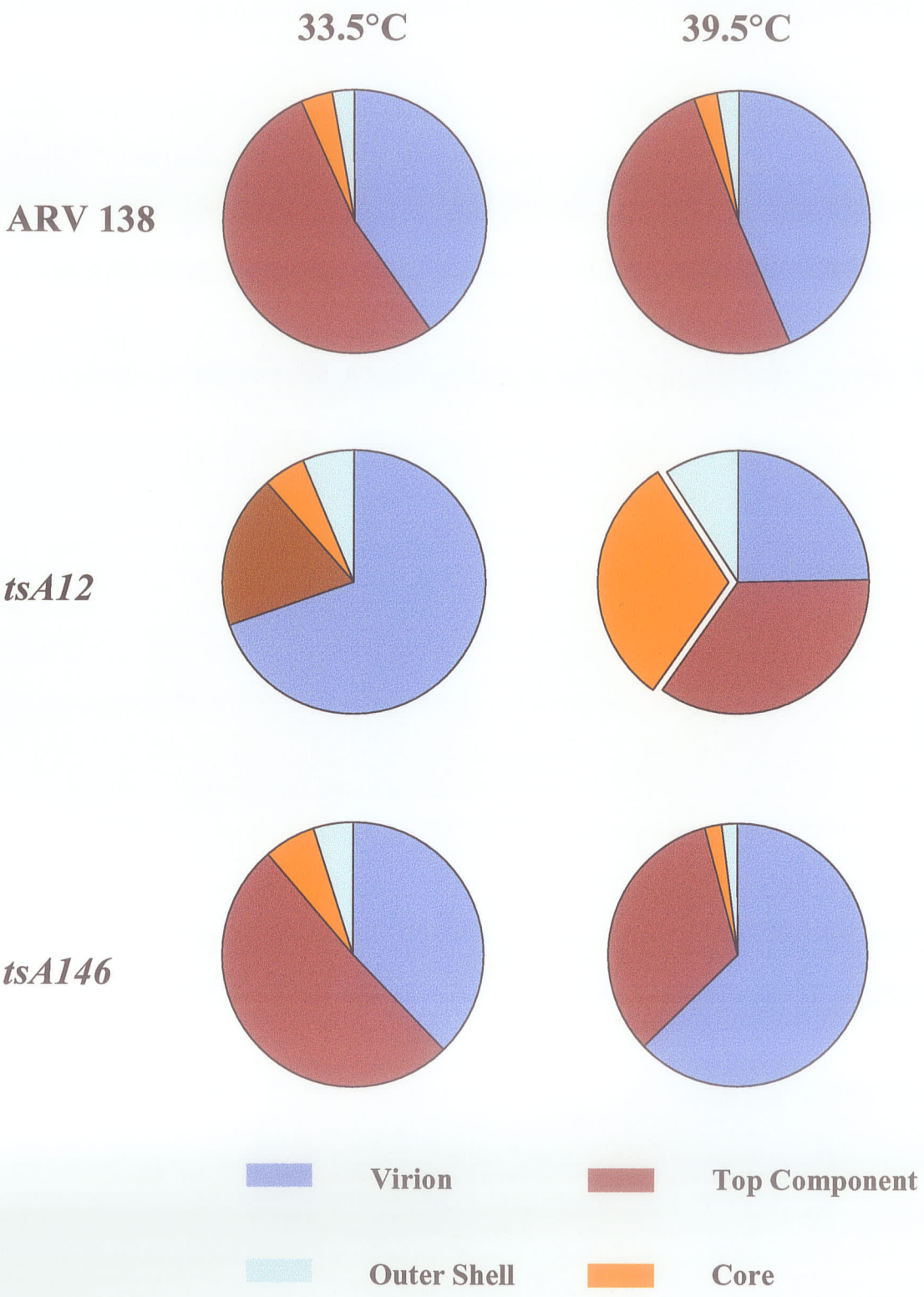
33.5°C
39.5°C
ARV 138
tsA12
tsA146
Virion
Top Component
Outer Shell
Core

Figure 3.2 Graphical representation of the proportion of types of particles produced by ARV 138, *tsA12*, and *tsA146* at permissive and nonpermissive temperatures.

Sample grids were prepared for ARV 138, *tsA12*, and *tsA146* as described in Materials and Methods. The relative proportions of structures produced by *tsA12*, *tsA146* and wild-type ARV138 at both permissive and nonpermissive temperatures were determined by direct particle counting of whole-cell lysates in 5 non-adjacent grid squares at magnifications between 30,000× and 70,000× using an electron microscope. Results are the average of three separate experiments.

was virion (70%) and top component comprised 19% of the particles produced. There was a trend toward increased proportions of top component and outer shells at the restrictive temperature. The proportion of core-like particles produced by *tsA12* increased significantly from 5% at the permissive temperature to 31% at the nonpermissive ($p < 0.0001$) (Table 3.1). Unlike *tsA12*, the mutant *tsA146* exhibited a significant increase in complete virions ($p < 0.0001$) and a significant decrease in top component ($p < 0.0001$) at 39.5°C compared to cells infected with ARV 138 and grown at the same temperature (Table 3.1).

3.1.3 Determination of localization of *ts* lesion in *tsA12*

3.1.3.1 SDS-PAGE analysis of ARV176 × *tsA12* reassortants

A total of 15 reassortant clones previously generated from mixed infection of ARV176 and *tsA12* were selected and amplified as described in Materials and Methods. The genome segments of these clones were resolved in 12.5% SDS-PAGE and their electropherotype profiles were compared with those of their parents. All clones were confirmed as reassortants.

3.1.3.2 Reassortant mapping of *tsA12*

To confirm the gene responsible for *ts* phenotype seen in *tsA12* at nonpermissive temperature, reassortant mapping of *tsA12* was performed. An EOP assay was used to test temperature sensitivity for each reassortant. Each *ts* clone was determined to have an EOP value of at least one order of magnitude lower than the wild-type ARV176 EOP value whereas each non-*ts* clone was defined as having an EOP value within one order of magnitude of the EOP value of wild-type. Thus, 6 reassortants were conformed as *ts*

clones from a total of 15 reassortants selected. 15 reassortants were divided into two panels: those reassortants that have the *ts* phenotype similar to mutant parent *tsA12* were arranged into top panel and those that have the non-*ts* phenotype similar to wild-type parent ARV176 were placed into bottom panel (Table 3.2). All *ts* clones had their S2 genome segment come from *tsA12*, whereas all non-*ts* clones had their S2 genome segment derive from ARV176. The remaining nine gene segments were randomly distributed. This indicates that the *tsA12 ts* lesion resides within the S2 gene segment, which confirms previous mapping.

3.1.4 Sequence analysis of the *tsA146* S2 gene

tsA146 phenotypically differ from *tsA12*, suggesting that the mutations in the S2 genes of the two viruses are different. To obtain direct evidence that phenotypic differences observed at nonpermissive temperature between the two mutants are due to the different alterations present within the protein, the S2 gene of *tsA146* was sequenced and the resulting protein primary structure was determined and compared with those of wild-type ARV 138 and *tsA12*. The sequence of the *tsA146* S2 gene was found to contain two nucleotide alterations as compared to parental ARV 138 S2 gene. These changes are C to U transitions at nucleotide positions 178 and 884, which lead to predicted proline to serine and threonine to isoleucine replacements at amino acid positions 55 and 290, respectively (Table 3.3 and Figure 3.3).

Hydropathy is a measure of the hydrophobic character of an amino acid. The hydrophobicity of the amino acids determines where the amino acid will be located in the final structure of the protein (Kyte and Doolittle, 1982). In globular proteins, the hydrophobic amino acids are more likely to be found on the inside of the protein, away

Table 3.2 Electropherotypes and efficiency of plating (EOP) values of ARV176 × *tsA12* reassortants

Clone	Electropherotype										EOP[a]
	L1	L2	L3	M1	M2	M3	S1	S2	S3	S4	
125	A[b]	A	7	A	A	7	7	A	7	7	0.00000640
ts A12	A	A	A	A	A	A	A	A	A	A	0.0000698
131	7	7	7	7	A	A	A	A	A	A	0.000110
160	7	7	7	A	7	7	7	A	A	7	0.000156
187	A	A	A	7	A	A	A	A	A	A	0.000160
192	A	A	7	7	A	A	A	A	A	A	0.000425
151	A	7	7	7	7	A	7	A	A	7	0.00160
64	A	7	7	A	A	A	A	A	A	A	0.00213
194	7	7	7	7	7	7	7	7	A	7	0.978
215	7	7	7	7	7	A	7	7	7	7	0.742
30	7	A	7	7	A	7	7	7	7	A	0.666
ARV176	7	7	7	7	7	7	7	7	7	7	0.588
148	7	A	7	7	A	A	7	7	7	7	0.548
243	7	7	7	7	A	7	7	7	7	7	0.426
65	7	7	7	7	A	A	7	7	7	7	0.316
229	A	7	7	7	A	7	A	7	7	A	0.218
159	7	7	7	7	7	7	A	7	7	7	0.147
169	7	7	7	7	A	7	7	7	7	A	0.130
Exceptions	3	6	6	4	8	5	4	0	2	6	

[a] EOP, efficiency of plating, (titer at 39.5°C) ÷ (titer at 33.5°C).

[b] A, Parental origin of gene. A, *tsA12*; 7, ARV176.

Table 3.3 Identified mutations in *tsA146* S2 gene

Base no.	AA[a] no.	Type of mutation	Codon change	AA[a] change	Polarity change[c]
178	55	transition	CCT to TCT	P[b] to S[b]	+0.8 (-1.6 to -0.8)
884	290	transition	ACC to ATC	T[b] to I[b]	+5.2 (-0.7 to 4.5)

[a] Amino acid.

[b] P, proline; S, serine; T, threonine; I, isoleucine.

[c] Based on the hydropathy index of amino acids (Kyte and Doolittle, 1982).

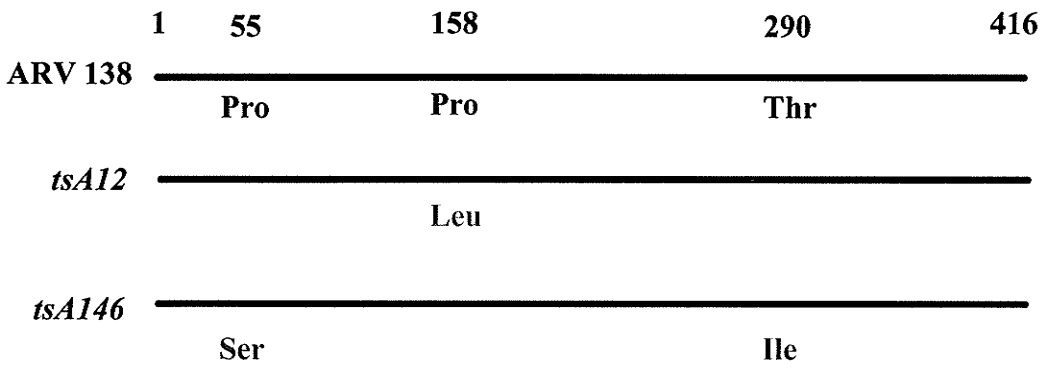

Figure 3.3 Alterations in deduced amino acid sequences of S2 gene product.

Mutated residues in temperature-sensitive mutants (*tsA12* and *tsA146*) are colour coded to distinguish the amino acids in corresponding wild-type ARV 138. Amino acid positions are numbered above the sequences.

from the water in the cytosol, while the hydrophilic amino acids are more likely to be found on the outside of the protein, interacting with the water in the cytosol. Kyte and Doolittle had assigned a hydropathy index to each amino acid based on water-vapor transfer free energies and interior-exterior distribution of side-chains (Kyte and Doolittle, 1982). Each amino acid is given a hydrophobicity score between -4.5 and 4.5. A score of 4.5 is the most hydrophobic while a score of -4.5 is the most hydrophilic. Based on the hydropathy index of amino acids (Kyte and Doolittle, 1982), the amino acid change at position 55 in the *tsA146* σA protein results in an increase from -1.6 to – 0.8 while the amino acid change at position 290 results in an increase from -0.7 to 4.5 (Table 3.3). Thus the mutated residue at position 55 is predicted to locate on the outside of the σA protein whereas the mutated residue at position 290 is predicted to reside on the inside of the protein.

Alignments of known amino acid sequences of ARV and MRV σ core proteins indicate that Thr_{290} is conserved while Pro_{55} is not (Duncan, 1999). This suggests that amino acid 290 may play an important role in protein function. Thus it may be the amino acid responsible for the phenotypic difference.

3.1.5 Structural locations of the mutations in *tsA12* and *tsA146* σA proteins

The S2 gene of the *tsA12* has previously been sequenced in our lab. The *tsA12* S2 gene contains one nucleotide alteration, which is a cytosine to uracil transition at nucleotide position 488. This nucleotide alteration leads to a proline-to-leucine substitution at amino acid position 158 in the σA protein (Figure 3.4C). The 3-dimentional structure of ARV is currently unknown, but analyses of known MRV and

ARV (Duncan, 1999) sequences suggest regions of high homology, which suggests the cognate proteins are folded similarly. Thus, the MRV crystal structure can probably be used as an important structural framework into which ARV structural results can be modeled.

Amino acid alignments of major core proteins of ARV σA and MRV σ2 suggest that Pro_{55}, Pro_{158}, and Thr_{290} in ARV σA protein correspond to amino acid positions 56, 160, and 292 in MRV σ2 protein, respectively. Thus, the locations of mutated residues of *tsA12* and *tsA146* within major σ core protein may be depicted by using MRV core crystal structure. Analyses of MRV core crystal structure (Figure 3.4) suggest that (1) the Pro-to-Leu substitution is located in the middle of the σ core protein and lies directly under the outer surface of the σ core protein (Figure 3.4C), where it may stabilize interaction between the σ core protein and the outer capsid μ protein; (2) the replacement of Pro to Ser is located on the inner surface of the σ core protein (Figure 3.4C); (3) the change from Thr to Ile is buried (Figure 3.4C).

3.2 Determination of localization of *ts* lesion in *tsB31*

3.2.1 Identification of ARV176 × *tsB31* reassortants

Recombination group B comprises only one clone, *tsB31*. To determine the gene segment that contains the *ts* lesion in recombination group B, *tsB31* was crossed with wild-type ARV176 as described in Materials and Methods. A total of 309 progeny clones were picked and all clones were amplified twice in QM5 cells to generate P2 stocks, which were subsequently used for further amplification. Each progeny clone was subjected to viral genome extraction. Extracted progeny viral genomes were resolved in

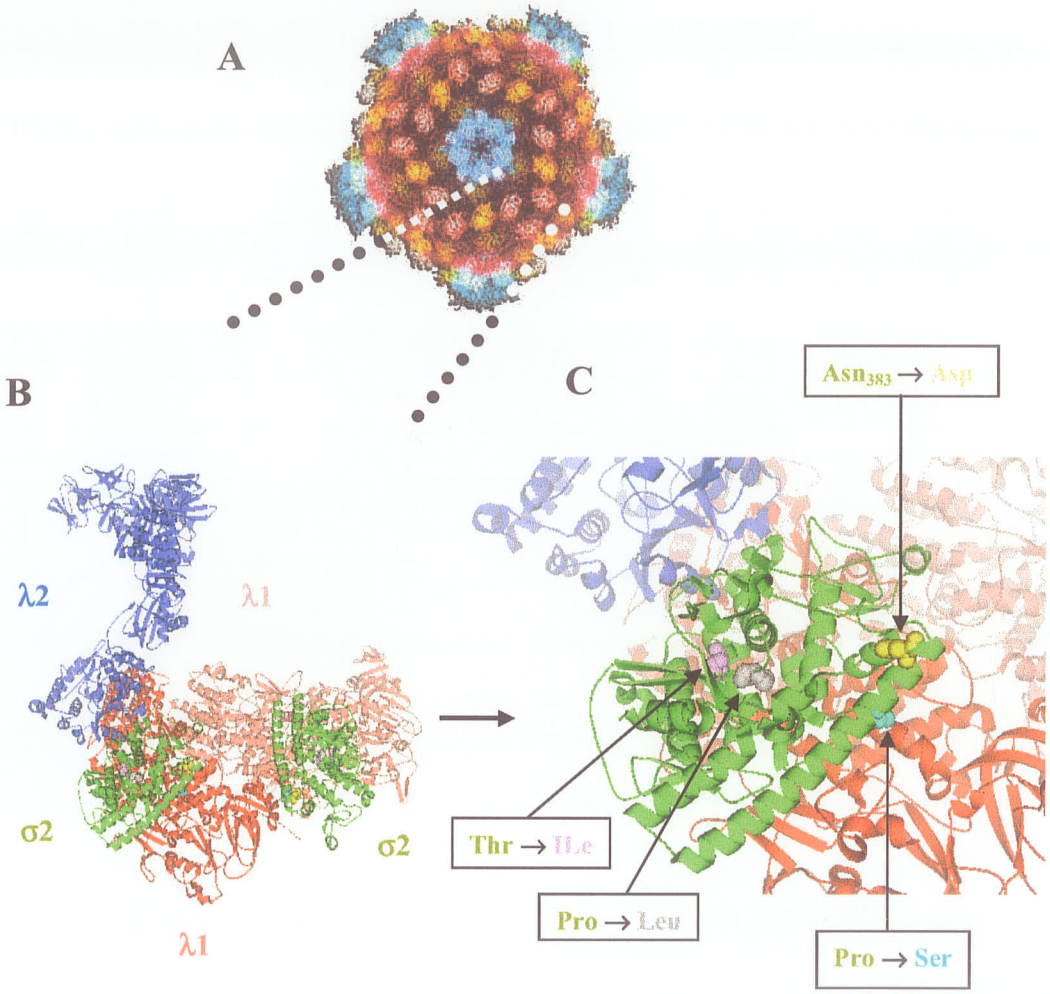
A
B
C
λ2
λ1
σ2
σ2
λ1
Asn383 → Asp
Thr → Ile
Pro → Leu
Pro → Ser

Figure 3.4 Locations of major σ core protein mutations of *tsA12* and *tsC447* in asymmetric unit of MRV core crystal structure.

(A) Crystal structure of MRV core (Reinisch *et al.*, 2000). (B) Blow-up of crystal "assymetric unit" (outlined in A), adapted and manipulated with PyMOL (DeLano, 2003). (C) Close-up of one of σ2 subunits from B showing locations of σ core protein MRV *tsC447* mutation (Asn → Asp) at amino acid position 383 (spheres, colored in yellow), ARV *tsA12* mutation (Pro → Leu) at amino acid position 158, and ARV *tsA146* mutations at amino acid positions 55 (Pro → Ser) and 290 (Thr → Ile) corresponding to amino acid positions 160 (spheres, colored in gray), 56 (spheres, colored in cyan), and 292 (spheres, colored in purple) in MRV σ2, respectively.

12.5% SDS-PAGE for reassortant identification. 12 clones had hybrid electropherotypes (Figure 3.5) and thus were determined as reassortants (reassortment efficiency = 4%).

One reassortant clone 208 appeared to lack a full-length S1 gene segment in SDS-PAGE. Two possibilities may account for this outcome. A small population of full-length S1 gene might exist but was undetectable under the experimental conditions and/or S1 gene truncation may have occurred during the course of generation of reassortants, which resulted in a smaller S1 gene segment that had run off the gel.

Clone 231 exhibited an aberrant mobility of its M2 gene segment on a polyacrylamide gel. For this reassortant, the designation for parental origin of the M2 genome segment was examined by analyzing the restriction fragment length polymorphism (enzymes *Eco*RV and *Sac*II) of a reverse-transcribed M2 fragment amplified by the polymerase chain reaction. The M2 restriction fragment length polymorphisms of *tsB31* and ARV 176 were analyzed in parallel. Restriction fragment length polymorphism data indicated that the M2 gene segment of clone 231 was derived from *tsB31* (Figure 3.6).

3.2.2 Determination of temperature sensitivity of ARV176 × *tsB31* reassortants

To determine temperature sensitivity of each reassortant generated from mixed infection of ARV 176 and *tsB31*, an EOP assay was repeatedly carried out three or four times on different days as described in Materials and Methods. 7 reassortant clones exhibited their average EOP values at least one order of magnitude lower than the wild-type ARV176 average EOP value and thus were determined as being temperature sensitive. By contrast, 5 reassortants clones had their average EOP values within one order of magnitude of the average EOP value of wild-type ARV176 and thus were

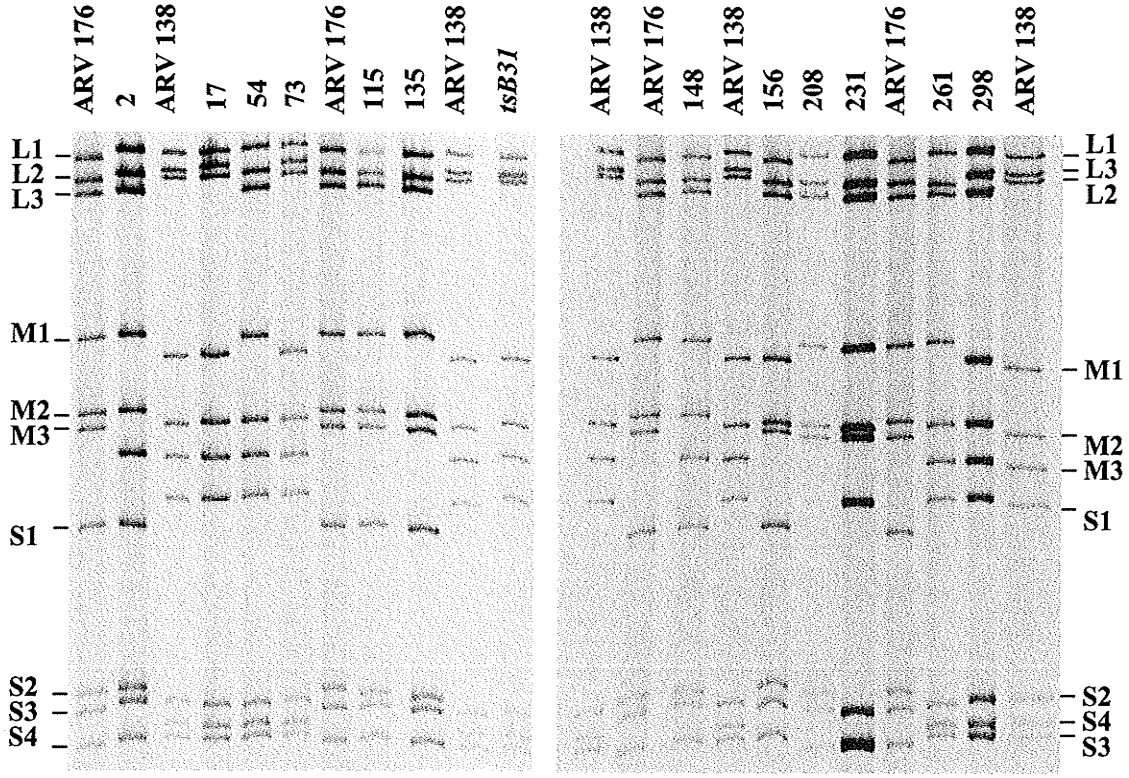

Figure 3.5 Electropherotyping of ARV 138, ARV176, *tsB31*, and reassortants generated from an ARV 176 × *tsB31* co-infection.

QM5 cells were infected with wild-type ARV 138, ARV 176, *tsB31*, and indicated reassortants. dsRNA genome segments were extracted, resolved in 12.5% SDS-PAGE, and stained with ethidium bromide. *tsB31* which was derived from mutagenesis of ARV 138 has same electropherotype with its parent ARV 138. The parental origins of reassortant genome segments are identified by comparing electropherotypes of ARV 138 and ARV 176.

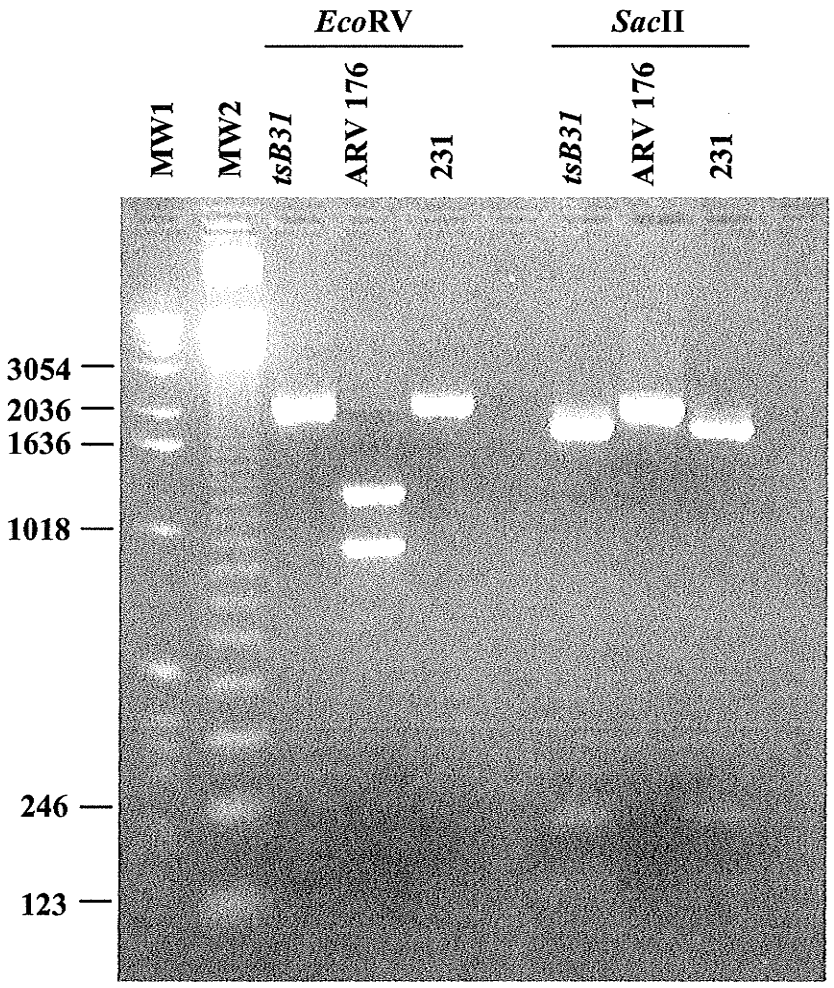

Figure 3.6 Restriction profiles of the M2 gene segments of avian reovirus wild-type strain 176, mutant *tsB31*, and ARV 176 × *tsB31* reassortant clone 231.

Genomic RNA of ARV 176, *tsB31*, and clone 231 were extracted. The M2 gene segments were reverse-transcribed, and amplified as described under Materials and Methods. Each of the resulting DNA fragments (2157 bp) was separately digested with *Eco*RV and *Sac*II. The digestion products were run on an agarose gel in parallel with molecular weight markers 1 Kb DNA Ladder (MW1) and 123 bp DNA Ladder (MW2).

determined as non-*ts* reassortant clones.

3.2.3 Reassortant mapping of *tsB31*

The identified reassortants from above were arranged into two panels according to their EOP ratios (Table 3.4). The top panel represents the reassortants that were identified as *ts* clones whereas bottom panel includes all reassortants that were non-*ts* clones. The top panel of reassortants that behaved like *tsB31* all had their M2 gene segments derived from *tsB31* and the bottom panel of reassortants that behaved like ARV176 all had their M2 gene segments come from ARV176 with the exception of clone 231. Each of the other nine gene segments was randomly associated with respect to temperature sensitivity. This indicates that the M2 gene is responsible for *ts* phenotype seen in *tsB31* and the *ts*-like reassortants. To determine statistical significance that the M2 gene is associated with *ts* phenotype, a Mann-Whitney test was carried out. The Mann-Whitney test, also called the rank sum test, is a nonparametric test that compares two unpaired groups. In this case, averaged EOP values of all reassortants were used as determinants to test the contribution of any single gene in the reassortant map. The Mann-Whitney test confirms that the M2 gene contains the *ts* lesion, with a probability of 0.006 (Table 3.4). The Mann-Whitney test also indicates that the M1 gene may contain a lesion, with a probability of 0.042 (Table 3.4).

3.3 Analysis of S1 gene truncation in some ARV clones

During the course of screening of ARV reassortants, some clones appeared to lack a full-length S1 gene segment in SDS-PAGE, but to be capable of propagation. For

Table 3.4 Electropherotypes and efficiency of plating (EOP) values of ARV176 × *tsB31* reassortants

Clone	Electropherotype										EOP[a]	SD[d]
	L1	L2	L3	M1	M2	M3	S1	S2	S3	S4		
73	B[b]	7	B	B	B	B	B	B	B	B	0.0007	0.000774
156	7	7	7	B	B	7	7	7	7	7	0.0014	0.00126
208	B	7	7	7	B	7	×[c]	7	7	7	0.003	0.00302
261	B	7	7	7	B	B	B	B	B	B	0.00411	0.00191
298	B	B	7	B	B	B	B	B	B	B	0.0053	0.000743
tsB31	B	B	B	B	B	B	B	B	B	B	0.0057	0.00398
54	B	B	7	7	B	B	B	B	B	B	0.0077	0.00767
17	B	7	B	B	B	B	B	B	B	B	0.0242	0.0179
148	7	7	7	7	7	B	7	7	7	7	0.242	0.0650
135	7	7	7	7	7	7	7	B	7	7	0.333	0.194
2	B	B	7	7	7	B	7	7	7	7	0.447	0.304
115	7	7	7	7	7	7	7	B	7	7	0.584	0.340
231	B	7	7	7	B	7	B	B	B	7	0.596	0.299
ARV176	7	7	7	7	7	7	7	7	7	7	0.953	0.595
Exceptions	3	5	5	3	1	4	2	5	3	2		
Mann-Whitney test p value	0.2398	0.9451	0.2912	0.042	0.006	0.2824	0.1375	0.8981	0.3176	0.0813		

[a] EOP, efficiency of plating, (titer at 39.5°C) ÷ (titer at 33.5°C).

[b] B, Parental origin of gene. B, *tsB31*; 7, ARV176.

[c] X, S1 gene segment absence.

[d] SD, Standard deviation based on three or four experiments.

[e] B, gene segment exhibits an aberrant mobility in 12.5% polyacrylamide gels and parental origin was identified by restrication fragment length polymorphism analysis.

example, 5 clones, named 29, 42, 61, 129, and 132 were generated from *tsB31* × ARV 176 cross and identified not to contain a full-length S1 gene. ARV S1 genome segment is 1643 base pairs (bp) and encodes three polypeptides from three sequential, partially overlapping open reading frames (ORFs) (Figure 3.7) (Bodelon *et al.*, 2001; Shmulevitz *et al.*, 2002). Proteins p10 and p17, which are specified by ORF1 and ORF2, respectively, are nonstructural proteins which associate with cell membranes, whereas ORF3 directs the synthesis of protein σC, a structural protein responsible for cell attachment (Bodelon *et al.*, 2001; Shmulevitz *et al.*, 2002). The p10 protein is responsible for the syncytium-inducing property (Shmulevitz and Duncan, 2000; Shmulevitz *et al.*, 2003), while the function of p17 is currently unknown. Maintenance of functional S1 gene products is obviously important for viral propagation. To understand the phenomena that these clones associated with lack of a full-length S1 gene are capable of propagation, clones 29, 42, 61, 129, and 132 were characterized.

3.3.1 Electrophoretic analysis of viral RNA

Clones 29, 42, 61, 129, and 132 which were generated from co-infection of *tsB31* and ARV 176 were amplified to the third passage and then subjected to genome extraction. The dsRNA of each clone was loaded into wells of sodium dodecyl sulfate polyacrylamide gel and electrophoresed at 12 mA for 20 hours instead of routine electrophoresis of 66 hours at 12 mA and then stained with ethidium bromide. These clones appeared to lack a full-length S1 gene but contained an extra band with an estimated size < 300 base pairs (bp) (Figure 3.8). The parental origins of other 9 gene segments of these clones were assigned to *tsB31*.

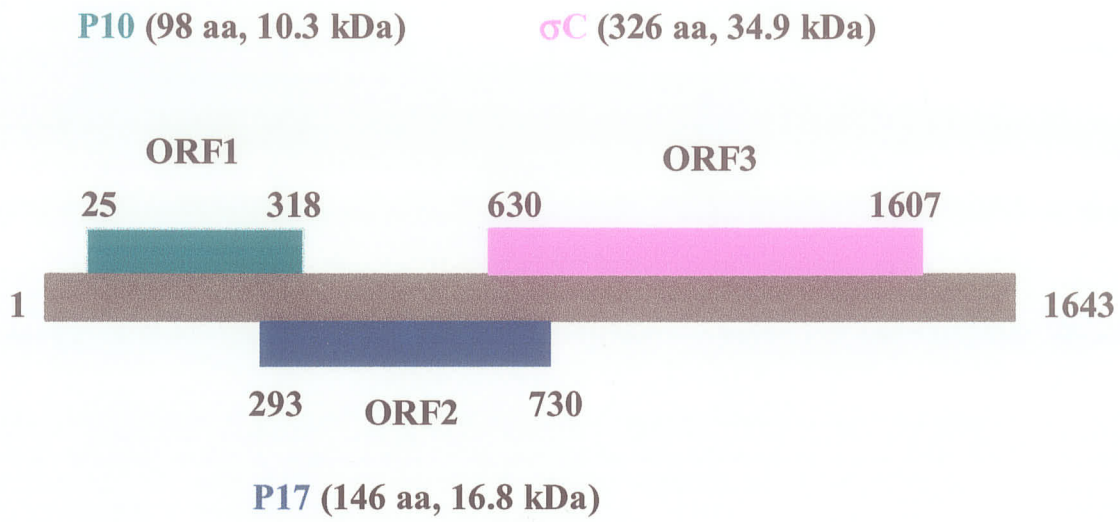

Figure 3.7 Gene arrangement of the tricistronic S1 genome segment of avian reovirus.

The arrangement of 3 predicated open reading frames (ORF) present in the ARV 138 S1 genome segment is depicted. The positions of the start and stop codons are indicated at the ends of the corresponding ORFs. The name, number of amino acid residues, and molecular mass of the proteins encoded by each ORF are indicated.

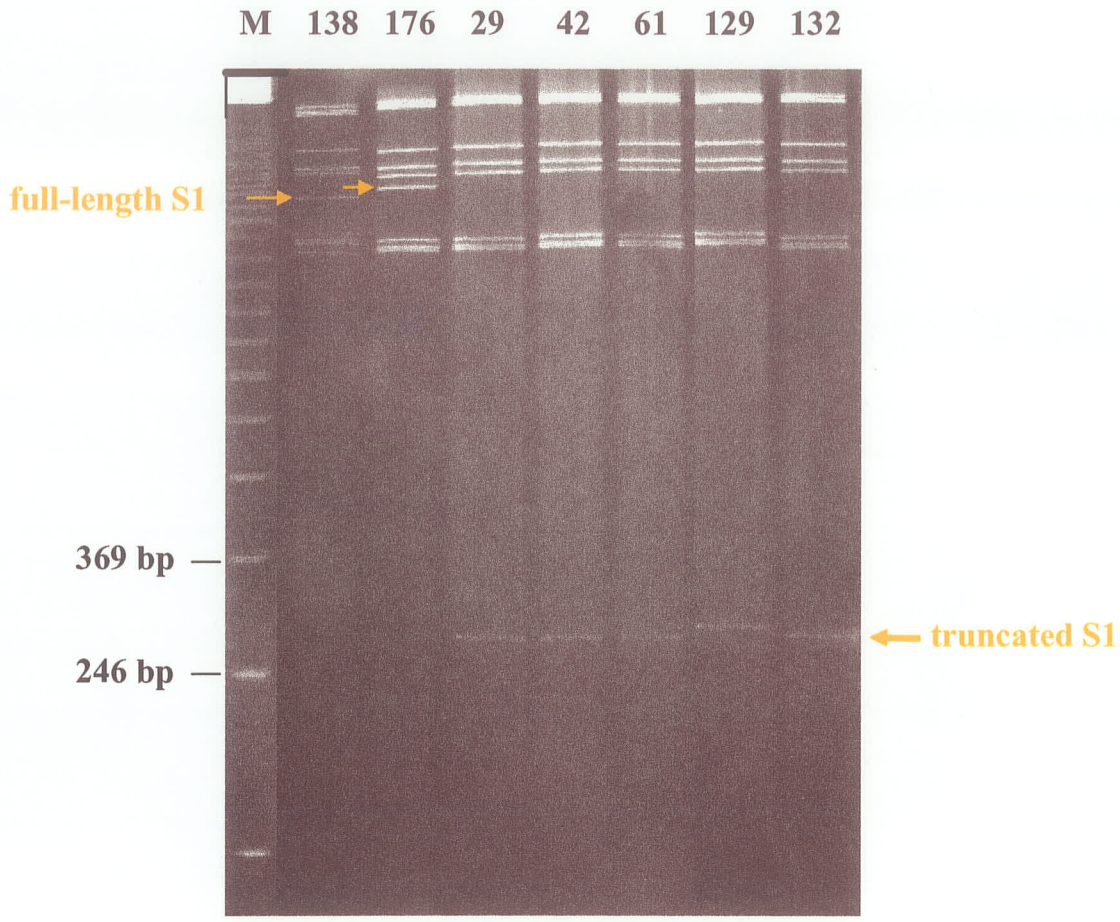

Figure 3.8 Electrophoretic analysis of truncated segments from *ts31*× ARV 176 clones.

The viral dsRNA extracted from infected QM5 cell lysates were separated by electrophoresis on 12.5% polyacrylamide gels for 20 hours, stained with ethidium bromide, and visualized and photographed under ultraviolet illumination. Lane M is 123 bp DNA ladder. ARV wild-types 138, 176, and 5 clones are indicated in each lane.

3.3.2 Sequence analysis of the S1 genome segment

The PCR assay offers the potential for rapid, sensitive, and precise molecular identification. To determine whether 5 co-infection progeny clones described above containing a small population of full-length S1 segments, molecular characterization of these clones was performed. 5 clones were amplified and gradient purified and their dsRNAs were extracted. Primers corresponding to 5' end and 3' end of plus strand S1 segment were designed and used to amplify S1 genome segments of 5 clones by RT-PCR as described in Materials and Methods. The PCR products were subjected to agarose gel electrophoretic analysis (Figure 3.9). While the S1 segment of ARV 138 or ARV 176 was amplified as an expected full length, each of 5 clones' amplicon appeared to be smaller than 300 bp (Figure 3.9), which is consistent with the size seen in SDS-PAGE. These PCR products were further purified and sequenced and the sequences were compared to those of the intact S1 segments of ARV 138 and ARV 176 (GenBank numbers AF218359 and AF218358). The sequence comparison (Figure 3.10) showed that (1) all clones had S1 deletion derived from ARV 138, indicating that the novel bands seen in SDS-PAGE are truncated forms of *tsB31* S1 segment; (2) all clones had S1 segments of 228 nucleotides in length except clone 42, whose S1 was 230 nucleotides in length; (3) all S1 deletion segments conserved the 5' and 3' ends of the intact S1 segment; (4) the sequence from the 5' end was 105-119 nucleotides long and the sequence from the 3' end was 111-123 nucleotides long; (5) No nucleotide substitutions were observed from existing sequences when compared to ARV 138 S1 sequence; (6) the sequence coding for p17 protein was completely deleted and sequences coding for proteins p10 and σC were partially retained.

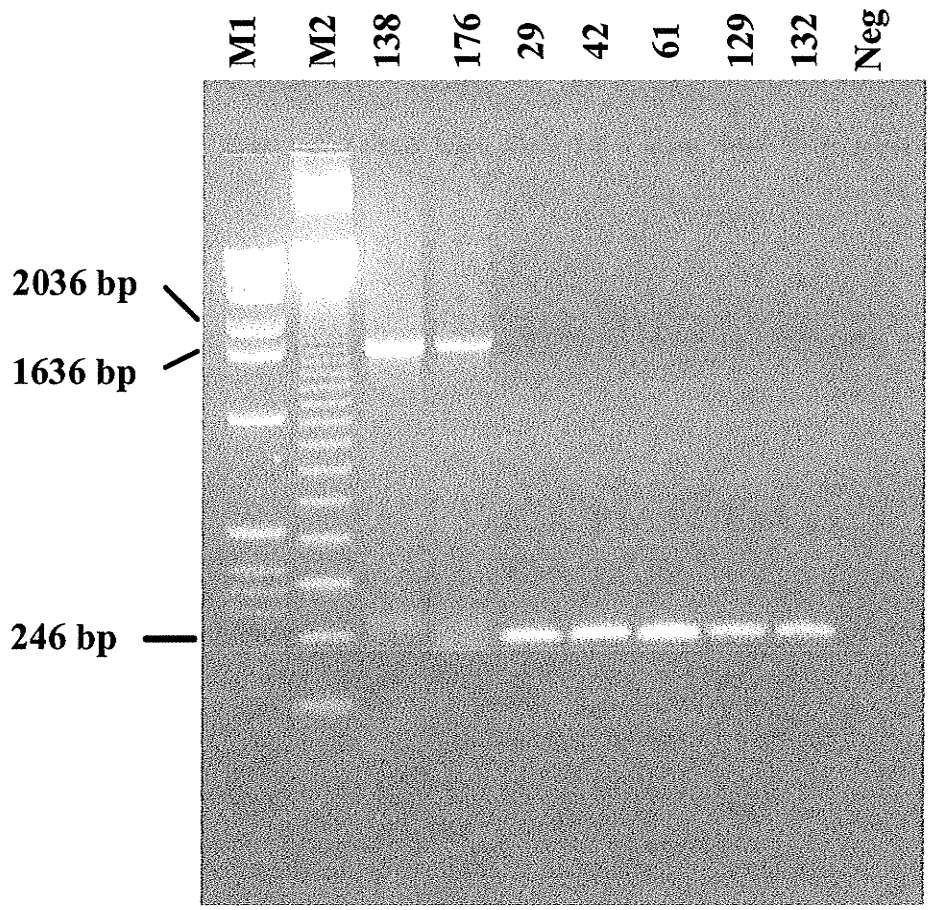

Figure 3.9 Agarose gel electrophoresis of PCR products produced by using full-length S1 genome segment target primers.

Lane M1, 1kb DNA ladder; lane M2, 123 bp DNA ladder. Each of ARV wild-types, 138, 176 was amplified as full-length S1 segment and each of 5 mutant clone's amplicon appears to be smaller than 300 bp. Last lane indicates template-free negative control.

```
138 GCTTTTTCAATCCCTTGTTTGTCGATGCTGCGTATGCCTCCCGGTTCGTG
176 GCTTTTTCAATCCCTTGTTCGTCGATGCTGCGTATGCCTCCCGGTTCGTG
 42 GCTTTTTCAATCCCTTGTTTGTCGATGCTGCGTATGCCTCCCGGTTCGTG
 29 GCTTTTTCAATCCCTTGTTTGTCGATGCTGCGTATGCCTCCCGGTTCGTG
 61 GCTTTTTCAATCCCTTGTTTGTCGATGCTGCGTATGCCTCCCGGTTCGTG
129 GCTTTTTCAATCCCTTGTTTGTCGATGCTGCGTATGCCTCCCGGTTCGTG
132 GCTTTTTCAATCCCTTGTTTGTCGATGCTGCGTATGCCTCCCGGTTCGTG
                              M  L  R  M  P  P  G  S  C

138 TAACGGTGCAACAGCTATCTTTGGTAACGTCCATTGTCAGGCGGCTCAAA
176 TAACGGTGCGACTGCTGTATTTGGTAACGTTCATTGTCAGGCAGCTCAAA
 42 TAACGGTGCAACAGCTATCTTTGGTAACGTCCATTGTCAGGCGGCTCAAA
 29 TAACGGTGCAACAGCTATCTTTGGTAACGTCCATTGTCAGGCGGCTCAAA
 61 TAACGGTGCAACAGCTATCTTTGGTAACGTCCATTGTCAGGCGGCTCAAA
129 TAACGGTGCAACAGCTATCTTTGGTAACGTCCATTGTCAGGCGGCTCAAA
132 TAACGGTGCAACAGCTATCTTTGGTAACGTCCATTGTCAGGCGGCTCAAA
    N  G  A  T  A  I  F  G  N  V  H  C  Q  A  A  Q  N
                   V
138 ATACTGCCGGCGGCGACTTGCAAGCTACCTCATCCATAATTGCCTATTGG
176 ACACGGCAGGTGGTGATTTGCAAGCTACGTCATCCATAATTGCATATTGG
 42 ATACTGCCGGCGGCGACTT----------------------------------
 29 ATACT----------------------------------------------
 61 ATACT----------------------------------------------
129 ATACT----------------------------------------------
132 ATACT----------------------------------------------
     T  A  G  G  D  L  Q  A  T  S  S  I  I  A  Y  W

138 //TCGCGTGTATTTACCATCACTTTCCCGACTGGTGGTGACGGTCCCGCAA
176 //TCACGTGTCTTCACAATTACTTTCCCAACCGGAGGTGATGGTACAGCGA
 42 ----------ACCATCACTTTCCCGACTGGTGGTGACGGTCCCGCAA
 29 -TCGCGTGTATTTACCATCACTTTCCCGACTGGTGGTGACGGTCCCGCAA
 61 -TCGCGTGTATTTACCATCACTTTCCCGACTGGTGGTGACGGTCCCGCAA
129 -TCGCGTGTATTTACCATCACTTTCCCGACTGGTGGTGACGGTCCCGCAA
132 -TCGCGTGTATTTACCATCACTTTCCCGACTGGTGGTGACGGTCCCGCAA
    //S  R  V  F  T  I  T  F  P  T  G  G  D  G  P  A  N
                                                  T
138 ATATCCGTTTCCTAACCGTGCGTACCGGCATCGACACCTAAGGTGTGGCG
176 ACATTCGTTCCTTGACCGTGCGTACCGGCATCGACACCTAAGGTGTGGCG
 42 ATATCCGTTTCCTAACCGTGCGTACCGGCATCGACACCTAAGGTGTGGCG
 29 ATATCCGTTTCCTAACCGTGCGTACCGGCATCGACACCTAAGGTGTGGCG
 61 ATATCCGTTTCCTAACCGTGCGTACCGGCATCGACACCTAAGGTGTGGCG
129 ATATCCGTTTCCTAACCGTGCGTACCGGCATCGACACCTAAGGTGTGGCG
132 ATATCCGTTTCCTAACCGTGCGTACCGGCATCGACACCTAAGGTGTGGCG
     I  R  F  L  T  V  R  T  G  I  D  T  *
           S

138 CCGTACGGGGATTGGTTATTCATC
176 CCGTACGGGGATTGGTTATTCATC
 42 CCGTACGGGGATTGGTTATTCATC
 29 CCGTACGGGGATTGGTTATTCATC
 61 CCGTACGGGGATTGGTTATTCATC
129 CCGTACGGGGATTGGTTATTCATC
132 CCGTACGGGGATTGGTTATTCATC
```

Figure 3.10 Alignment of the S1 segment cDNA sequences of ARV 138, ARV176, and 5 deletion mutants.

The S1 genome segment nucleotide sequences of 5 deletion mutants are aligned with S1 nucleotide sequences of ARV 138 and ARV 176. The nucleotides that are not conserved in the alignment are colored in red. Truncated portion of the S1 segment sequence from full-length S1 segment is indicated by symbol // or dashes. Deduced amino acid sequences are presented. Start codon of p10 protein is indicated in blue. Asterisk indicates the location of the termination codon of the σC protein. The locations of primers used for sequencing are underlined.

3.3.3 Identification of temperature sensitivity

As the 5 S1 deletion clones are actually derivatives of *tsB31*, they are expected to be *ts*. EOP analyses of clones 29, 42, 61, 129, and 132 were conducted twice on different days. All clones were confirmed to be temperature sensitive as they had an EOP value of 0.001 or lower (Table 3.5).

3.3.4 Analysis of replicative ability

ts mutants can grow at a low temperature but not at a high temperature, in contrast to wild-type virus, which grows at both temperatures. To determine if the S1 truncation has an impact on replication of 5 *ts* clones at permissive temperature, the growth capacity of 5 clones was examined. Subconfluent QM5 cell monolayers were infected with individual clone or wild-type ARV 138 at an MOI of 10 for 1 hour at room temperature, then the inoculum was removed and cells were supplemented with incubation Medium 199 and incubated at 33.5°C. At different times post-infection, cells were lysed and the concentration of infectious viral particles was determined by plaque assay. The growth curves obtained (Figure 3.11) show that the replications of the S1 deletion clones were not reduced relative to titers obtained from ARV 138 infection. The production of infectious viral particles was 1- to 9-fold more than that of ARV 138 infection at the corresponding times post-infection.

Table 3.5 Efficiency of plating (EOP) values of S1 deletion mutants.

Clone	Trial 1	Trial 2	Average	Standard Deviation
29	0.000909	0.000873	0.000891	0.0000255
42	0.00127	0.0117	0.00649	0.00738
61	0.00472	0.00935	0.00704	0.00327
129	0.000741	0.0223	0.0115	0.0152
132	0.00129	0.0243	0.0128	0.0163
ARV 176	0.604	0.55	0.577	0.0382

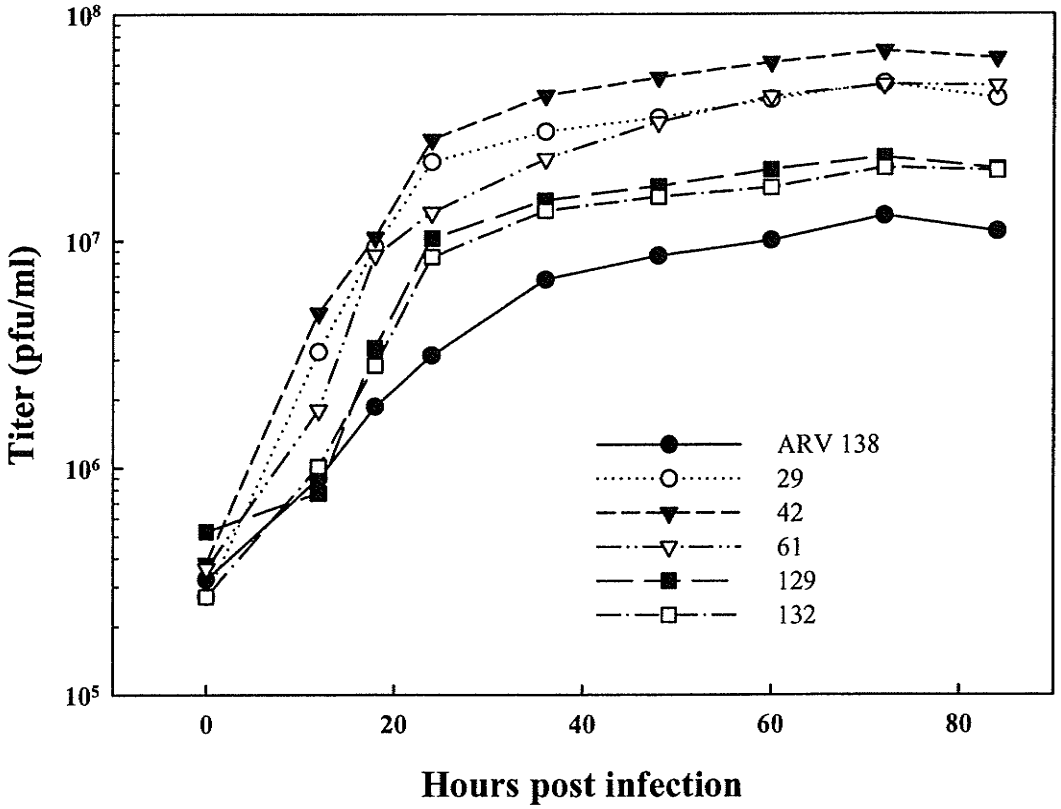

Figure 3.11 Growth curves of wild-type ARV 138 and 5 S1 deletion mutants. Subconfluent monolayers of QM5 cells were incubated with 10 PFU/cell of ARV 138, clones 29, 42, 61, 129, or 132 for 1 hour at room temperature. After removal of the virus input and subsequent washing of the plates, growth Medium 199 was added, and incubation proceeded for the times indicated. Infections were harvested by two freeze-thaw cycles and sonication. The concentration of infectious virus particles was determined by plaque assay.

CHAPTER 4 DISCUSSION

4.1 Characterization of the group A mutants

tsA12, prototype of the group A mutant, was further characterized and compared with mutant *tsA146* and unmutagenized parent ARV 138. Although the *ts* lesion of *tsA12* and *tsA146* is assumed to reside in the same gene based on recombination assay, two lines of evidence indicate that mutations in *tsA12* and *tsA146* are different and cause different phenotypic responses. First, analyses of replicative abilities of two mutants at various temperatures demonstrate that the production of infectious *tsA12* was markedly reduced at 37°C or higher (Figure 3.1F). Production of infectious *tsA146* progeny was also reduced at temperatures above 37°C, but *tsA146* replication was impaired to greater extents as the restrictive temperature was increased (Figure 3.1F). Obviously, *tsA12* mutation is more detrimental to *tsA12* replicating at a relatively high temperature compared to *tsA146* replication. Second, direct particle counting of *tsA12* and *tsA146* infected cell lysates reveals that *tsA12* but not *tsA146* mutant significantly produced core-like particles at the nonpermissive temperature (Table 3.1). The lesion of *tsA12* that results in the *ts* phenotype was confirmed to reside in the S2 gene by reassortant mapping experiments (Table 3.2). The mutations in the *tsA146* S2 gene were determined by sequence analysis, which proves that the different phenotypic responses between the mutants *tsA12* and *tsA146* are caused by different mutations in the S2 gene. Thus *tsA12* represents a novel assembly-defective mutant which is not able to assemble past the core.

The ARV S2 gene segment is 1324 bp long (Duncan 1999) and encodes major core protein σA. σA is a 45.5 kDa protein (Yin *et al.*, 2000) consisting of 416 amino

acids (Duncan 1999). This protein has been proposed to have similar structure/function with MRV major core protein σ2 (Yin *et al.*, 2000), which is also encoded by S2 gene. Thus, it is likely both σA and σ2 (Reinisch *et al.*, 2000) bind to the outer face of the core structure and act as a clamp to hold the core structure together. Although the protein sequences between ARV σA and the 3 serotypes (types T1L, T2J and T3D) of MRV σ2 have approximately 30% similarity, σA and σ2 share similar predicted secondary structure (Yin *et al.*, 2000). Moreover, it has been reported that both proteins of σA and σ2 have dsRNA-binding activity (Dermody *et al.*, 1991; Yin *et al.*, 2000), indicating an important role of this major core protein in reovirus transcription and replication or in packaging the viral genome segments during virion assembly. Previous studies have shown that ARV group A mutants (*tsA12* and *tsA146*) and their counterpart, MRV *tsC447*, whose mutation also maps to the S2 gene (Ramig *et al.*, 1978), exhibit an inability to produce progeny dsRNA (Cross and Fields, 1972; Ito and Joklik, 1972; Patrick *et al.*, 2001) and produce reduced amounts of protein at the nonpermissive temperature (unpublished data for ARV; Cross and Fields, 1972; Fields *et al.*, 1972). Thus, corresponding defects in the major σ core protein may have impacts on dsRNA production and protein synthesis under restrictive growth conditions. This also is consistent with the reduction in particle yield for *tsA12* and *tsA146* (Table 3.1), and is correlated to the observation of low level of progeny proteins produced in restrictive infection (unpublished data). However, the mechanism by which the major σ core protein is involved in these phenotypes is not understood and needs to be further investigated.

Interestingly, while ARV *tsA12* assembles core structures in restrictive infections (Table 3.1), ARV *tsA146* and the cognate MRV *tsC447* fail to produce cores but MRV

tsC447 does synthesize empty outer capsid structures at the nonpermissive temperature (Fields *et al.*, 1971; Matsuhisa and Joklik, 1974; Coombs *et al.*, 1994). Analysis of deduced protein sequences of ARV group A mutant S2 genes revealed that *tsA12* σA contains a single amino acid substitution (proline to leucine) at position 158, whereas *tsA146* σA have two amino acid substitutions (proline to serine and threonine to isoleucine) at positions 55 and 290, respectively (Figure 3.3). Although the detailed ARV core structure is not currently known, use of the available MRV core crystal asymmetric unit (PDB # 1EJ6) (Reinisch *et al.*, 2000) as a model predicts that the altered amino acid in *tsA12* lies under the outer surface of the σA protein (Figure 3.3C). This mutation might affect the distal side of the protein where it prevents condensation of outer capsid proteins onto the core, and thus may lead to alterations in particle distribution seen in *tsA12* at the nonpermissive temperature. A mutated residue at position 290 in *tsA146* σA also lies under the outer surface of the protein, but this mutation might affect the ability of the σA protein to interact with dsRNA at elevated temperature, promoting assembly of complete virions rather than top component structures. This explains the shift in proportion of particles produced from top component to complete virions (Table 3.1) and is consistent with our recent observation in thin section EM, where nucleic acid is seen as dense condensates at the periphery of the inclusions for restrictive temperature cultures.

The sequence of the comparable MRV *tsC447* mutant gene has been determined to contain several nucleotide alterations that lead to amino acid substitutions (Wiener *et al.*, 1989)(Figure 4.1). However, extensive genetic reversion analyses indicated that an asparagine to aspartic acid change at amino acid position 383 is most likely responsible for the failure of *tsC447* to assemble core particles at the nonpermissive temperature

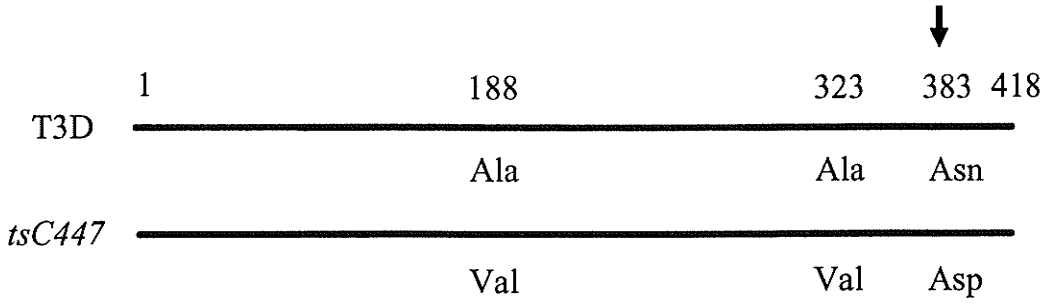

Figure 4.1 Alterations in predicted amino acid sequences of MRV S2 gene product in corresponding wild-type and *ts* mutant.

Three amino acid substitutions Ala-to-Val, Ala-to-Val, and Asn-to-Asp at amino acid positions 188, 323, and 383 in the *tsC447* major σ core protein are indicated. Amino acid positions are numbered above the sequences. Amino acid change responsible for *ts* phenotype is indicated by an arrow.

(Coombs *et al.*, 1994). The region of σ2 near or at Asp_{383} is positioned on the outer surface of the protein (Figure 3.4C). Thus, the introduction of a mutated residue in this region in the σ2 amino acid sequence appears to prevent σ2-σ2 interactions that would normally lead to core capsid assembly. Alignments of major σ core protein sequences of mammalian reoviruses, avian reoviruses, and Nelson Bay reoviruses revealed that residues Pro_{158} and Asn_{383} are conserved among the species (Duncan 1999), implying their structural importance. Thus mutations caused at one of these residues would result in structural instability and different mutations in the cognate major core proteins of MRV and ARV lead to different phenotypic responses. The comparative analyses of ARV *ts* mutant and its MRV *ts* mutant counterpart will not only allow us to expand our understanding of viral proteins, but should help to provide a more complete picture of assembly of these complex particles (Figure 4.2).

4.2 S1 deletion mutants

Some mammalian reoviruses that accumulate deletion mutants have been found to involve the L1, L2, L3, and M1 genome segments (Nonoyama *et al.*, 1970; Nonoyama and Graham 1970; Schuerch *et al.*, 1974; Ahmed and Graham, 1977; Ahmed and Fields 1981; Brown *et al.*, 1983; Zou and Brown 1992). To date, deletion events among avian reoviruses are reported to involve S1 gene segment (Ni and Kemp, 1992; 1994). The major features for most deletion mutants are that 1) they are generated during serial passage at high multiplicity; 2) they are defined as defective interfering particles because of their ability to interfere with the growth of complete virus by effectively competing for limiting essential replication factors; 3) their genomes or genome segments are usually grossly altered genetically but can still replicate and be assembled into progeny virus

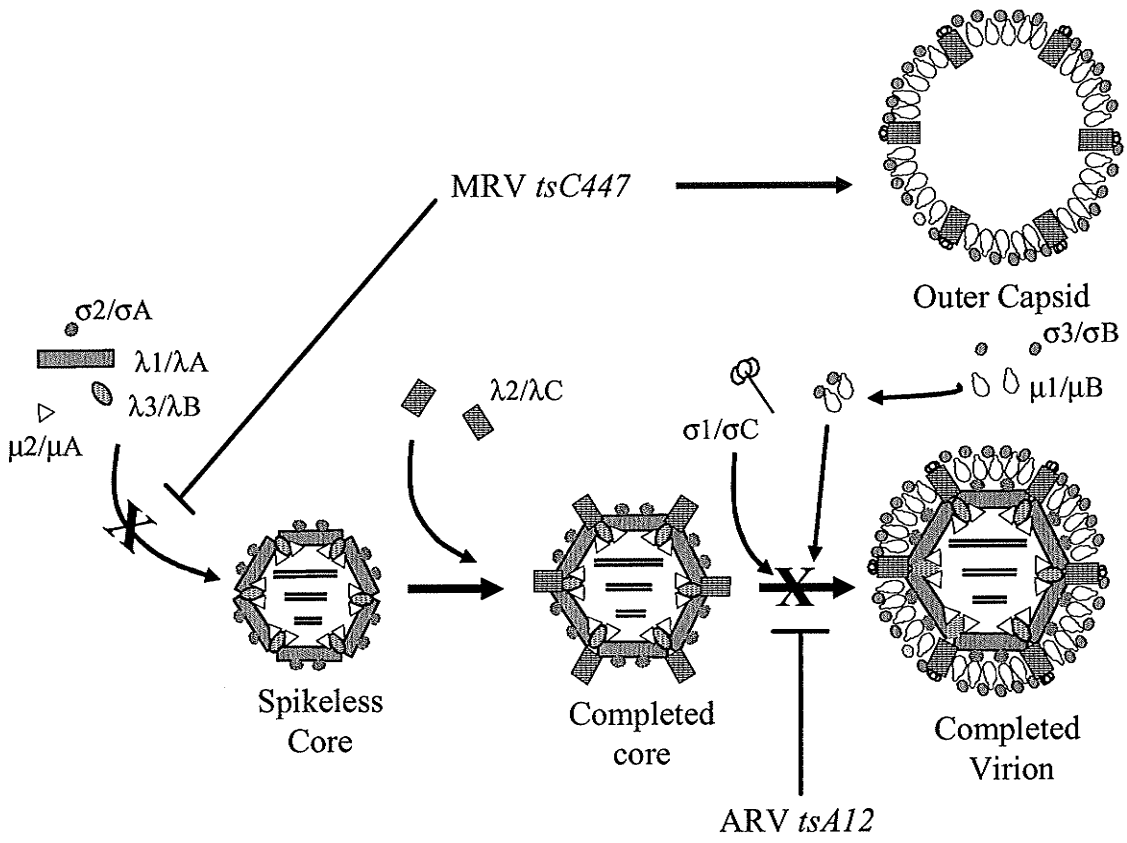

Figure 4.2 Proposed reovirus assembly pathways.

Locations and identities of the eight major structural proteins of the virus are indicated. Blocks mediated by ARV *tsA12* or MRV *tsC447* in the pathways are marked by ×.

with complement of helper virus.

Clones that lack an intact S1 gene segment are commonly observed in our lab during screening of ARV reassortants from mixed infections. These mixed infections were carried out by crossing wild-type ARV 176 with one of *ts* mutants derived from mutagenesis of wild-type ARV 138. Screening of reassortants by SDS-PAGE was conducted when plaque-derived clones have been amplified to the third passage at high multiplicity. Two types of S1 deletion clones, either reassortant or non-reassortant were found in our experiments. A panel of non-reassortant S1 deletion mutants (clones 29, 42, 61, 129, and 132) derived from ARV 176 × *tsB31* were chosen and analyzed. RT-PCR could detect <300 bp S1 fragments but not full-length S1 genome segments from gradient purified mutant particles. Sequence analyses of these S1 fragments revealed that they were derived from *tsB31* S1 genome segment and 86% portion of the segment was internally deleted. Nevertheless, all S1 truncated clones conserved their two terminal regions of S1 (105-119 nucleotides from 5' end and 111-123 nucleotides from 3' end), indicating that signals for replication and packaging were retained. To ensure replication and assembly of all 10 genome segments, each segment must maintain a dsRNA-dependent transcriptase promoter at the 3' end of the minus strand and an ssRNA-dependent replicase promoter at the 3' end of the plus strand as well as sequences necessary for assembly. In assembly, signals are required to identify a replica as being reoviral as well as being a specific genome segment. To date, the sequences of the four S class genome segments of ARV have been reported for ARV 138 and ARV 176 (Duncan, 1999). The 3'-terminal sequence UCAUC and 5'-terminal sequence GCUU are conserved in all S class genome segments presumably as well as in all L and M segments of ARV,

suggesting their role in recognizing viral genome. The segment-specific signal must be elsewhere since it serves to distinguish between segments. An attempt made in MRV to identify such signals failed (Antczak *et al.*, 1982). However it is possible to postulate that the nontranslated regions are likely to include sequences important for segment packaging from our S1 deletion sequence data. It seems to be a common feature that both terminal sequences of all viruses with segmented RNA genomes play critical roles in genome transcription, replication, and packaging (Nuss and Summers, 1984). Sequence analyses of a series of deleted M1 segments of MRV revealed that the minimum consensus sequences for 5'- and 3'- ends of the plus strand were 132 to 135 and 182 to 185 bases, respectively (Zou and Brown, 1992). In the studies of complete (Anzola *et al.*, 1987) and mutated (Xu *et al.*, 1989; Dall *et al.*, 1990) wound tumor virus (WTV), a member of the phytoreovirus genus in the family *Reoviridae*, it has been suggested that both terminal sequences were involved in genome replication and/or packaging. The terminal sequences conserved in all segments of WTV were responsible for distinguishing viral RNA from cellular RNA, whereas the segment-specific terminal sequences were involved in identifying a particular viral genome segment.

SDS-PAGE and sequence analyses showed that all genome segments of analyzed S1 deletion mutants were derived from *tsB31* (its *ts* lesion was mapped to the M2 gene); hence these S1 deletion clones are in fact double mutants that contain the *ts* lesion in the M2 gene and deletion mutation in the S1 gene. The *ts* phenotype of S1 deletion clones was also confirmed by EOP assay. In Ni and Kemp (1994)s' report, truncated S1 fragments generated by serial passage of the coinfection progeny of two ARV strains were defective interfering (DI) RNAs that compete or interfere with the full-length S1

genome segment during replication and/or packaging, i.e., serially passaged coinfection progeny contain DI particles that lack the intact S1 segment, but contain truncated S1 segment. Based on the phenomenon described by Ni and Kemp above, if truncated S1 segments generated in our experiment are DI RNAs, the corresponding clones from the third passage must have contained DI particles. These DI particles should actively inhibit replication of helper virus, i.e., *tsB31* during the "coinfection" (assumably *tsB31* and its DI particles), resulting in decrease of infectious titers. Unexpectedly however, a comparison of the growth curves between S1 deletion clones and wild-type ARV 138 demonstrated that the S1 deletion clones appeared to replicate efficiently at the permissive temperature throughout the growth cycle compared to replication of wild-type ARV 138. Thus two lines of evidence suggest that the truncated S1 genome segments generated in our experiment are indeed not DI RNAs: (i) S1 deletion clones were generated at lower passage rather than at higher passage; (ii) truncated S1 fragments did not show interfering property seen in DI RNAs as S1 deletion clones replicate efficiently at permissive temperature.

Among 10 genome segments of ARV, S1 genome segment represents only one genome segment that appears to be polycistronic, i.e., tricistronic. Three ORFs coding for fusion protein p10 (ORF 1), p17 (ORF2, function is not known), and cell attachment protein σC, are arranged in a sequential, partially overlapping fashion (Shmulevitz *et al.*, 2002). The majority of mRNAs that encode more than one gene product are usually bicistronic and contain ORFs that are either nested within each other (e.g. MRV S1 genome segment, Ernst and Shatkin, 1985) or overlap each other extensively (e.g. the polycistronic P/C mRNA of Sendai virus, Latorre *et al.*, 1998). The highly unusual

arrangement seen in the ARV S1 genome segment may lead to aberrant replication on this segment more easily than other 9 genome segments. This might be the reason why only S1 deletion event has been observed to date.

As S1 genome segment of analyzed clones was grossly truncated, it is impossible to predict that any functional proteins from within could be formed in the infection. Thus the great amount of non-infectious defective viruses would be generated, leading to a decrease in infectious titers. The contradictory phenomenon that the S1 deletion mutants generated in our experiment are infectious and capable of undergoing productive infection raises a question, how can these mutants enter the cells without cell attachment proteins? The underlying mechanism, if any, is not understood and remains to be elucidated. However evidence has suggested that the cell attachment protein σC is not sufficient and/or required to promote the membrane interactions necessary for ARV entry (Duncan, 1996). ARV has employed an additional mechanism using major outer capsid protein μB to facilitate its entry (Duncan, 1996). The S1 deletion mutants that are capable of growth are not an only case of paradox seen in ARV. Our other study of ARV *ts* mutants showed that many *ts* mutants fail to produce progeny dsRNA but do synthesize progeny protein at the nonpermissive temperature of 39.5°C. Taken together, these paradoxes increase the need to study ARV replication in more detail.

4.3 Future directions

The overall objectives of this research are to continue to use the genetic tools of "reassortant mapping" and *ts* mutant characterization to better understand structure/function and assembly of avian reoviruses. *tsA12* and *tsA146* of the recombination group A exhibiting different phenotypic responses at nonpermissive temperature were demonstrated in this study. Sequence analysis of deduced amino acid of *tsA146* S2 gene revealed that mutations in *tsA146* differ from that of *tsA12*. This suggests

that different amino acid substitutions in the major σ core protein may have caused different conformational changes. The hypothesized differences in conformational change within the major core protein σA of mutants *tsA12* and *tsA146* can possibly be determined by mass spectrometric analysis. Briefly, parental wild-type virus and two mutants could be grown at both permissive and nonpermissive temperatures. Purified core particles from all sources could then be treated with a battery of proteases for various periods of time and the differences in the peptide maps of wild-type and two mutant particles could be analyzed by a mass spectrometer. Thus the molecular signals responsible for ARV assembly could be determined.

One of the most important aspects of our ARV studies is first to complete the gene assignments of each group of ARV mutants so we know what we are working with. Thus far genes that harbored the *ts* lesions from 7 recombination groups have been assigned for groups A and D and the mutation of group B has been mapped to the M2 gene segment with one exception in this study (Table 3.4). The clone 231 that contributes to this exception might be regrouped as a non-*ts* reassortant by increasing the restrictive temperature; therefore it could possibly be ruled out. Sequence analyses of the *tsB31* M2 gene as well as genes (M1, S1, and S4) that could possibly be associated with temperature sensitivity, could definitely conclude if the *tsB31 ts* lesion resides in the M2 gene. The M2 gene encodes major outer capsid protein μB, the equivalent of the MRV μ1 capsid protein. Like MRV μ1 protein, ARV μB has been proposed to associate with σB to form the bulk of the virion outer capsid and also interacts with core proteins λC and σA in virions (Van Regenmortel *et al.*, 2000). MRV μ1 protein has many important functions that appear to be involved in conferring particle stability on membrane

permeabilization (Hooper and Fields, 1996), virus entry (Sturzenbecker *et al*, 1987; Nibert and Fields, 1992; Lucia-Jandris, 1993; Tosteson *et al.*, 1993) and transcriptase activation (Drayna and Fields, 1982; Ewing *et al.*, 1985). The function of ARV μB has been determined to be involved in virus entry (Duncan, 1996) and other functions, if any, have yet to be determined. The next step after confirming the localization of the *ts* lesion in *tsB31* will be in examining morphological effect of the mutation and hopefully, a new assembly-defective mutant can be identified to help understanding of the role of μB in ARV assembly.

With S1 deletion mutants that were generated from coinfection of ARV 176 and *tsB31*, the phenomenon that the S1 deletion mutants paradoxically replicated to higher titers at permissive temperature without helper viruses remains to be explained. However, sequences of S1 gene segment identified from S1 deletion mutants may be used for reverse genetics to identify signals that control specific aspects of replication and assembly.

REFERENCES

Acs, G., Klett, H., Schonberg, M., Christman, J., Levin, D. H., Silverstein, S. C. (1971). Mechanism of reovirus double-stranded ribonucleic acid synthesis in vivo and in vitro. *J Virol.*, **8,** 684-689.

Ahmed, R., Fields, B. N. (1981). Reassortment of genome segments between reovirus defective interfering particles and infectious virus: Construction of temperature-sensitive and attenuated viruses by rescue of mutations from DI particles. *Virology,* **111,** 351–363.

Ahmed, R., Graham, A. F. (1977). Persistent infections in L cells with temperature-sensitive mutants of reovirus. *J Virol.*, **23,** 250-262.

Antczak, J. B., Chmelo, R., Pickup, D. J., and Joklik, W. K. (1982). Sequence at both termini of the 10 genes of reovirus serotype 3 (strain Dearing). *Virology,* **121,** 307-319.

Antczak, J. B. and Joklik, W. K. (1992). Reovirus genome segment assortment into progeny genomes studied by the use of monoclonal antibodies directed against reovirus proteins. *Virology*, **187,** 760-776.

Anzola, J. V., Xu, Z. K., Asamizu, T., Nuss, D. L. (1987). Segment-specific inverted repeats found adjacent to conserved terminal sequences in wound tumor virus genome and defective interfering RNAs. *Proc Natl Acad Sci U S A.*, **84,** 8301-8305.

Bartlett, N. M., Gillies, S. C., Bullivant, S., and Bellamy, A. R. (1974). Electron microscopy study of reovirus reaction cores. *J. Virol.* **14,** 315-326.

Barton, E. S., Forrest, J. C., Connolly, J. L., Chappell, J. D., Liu, Y. Schnell, F. J., Nusrat, A., Parkos, C. A. and Dermody, T. S. (2001). Junction adhesion molecule is a receptor for reovirus. *Cell*, **104,** 441-451.

Becker, M. M., Goral, M. I., Hazelton, P. R., Baer, G. S., Rodgers, S. E., Brown, E. G., Coombs, K. M., and Dermody, T. S. (2001). Reovirus sigmaNS protein is required for nucleation of viral assembly complexes and formation of viral inclusions. *J. Virol.*, **75**, 1459-1475.

Becker, M. M, Peters, T. R., and Dermody, T. S. (2003). Reovirus sigma NS and mu NS proteins form cytoplasmic inclusion structures in the absence of viral infection. *J Virol.*, **77**, 5948-5963.

Bisaillon, M., Bergeron, J., and Lemay, G. (1997). Characterization of the nucleoside triphosphate phosphohydrolase and helicase activities of the reovirus lambda1 protein. *J. Biol. Chem.*, **272**, 18298-18303.

Bisaillon, M. and Lemay, G. (1997a). Molecular dissection of the reovirus lambda1 protein nucleic acids binding site. *Virus Res.*, **51**, 231-237.

Bisaillon, M. and Lemay, G. (1997b). Characterization of the reovirus lambda1 protein RNA 5'-triphosphatase activity. *J. Biol. Chem.*, **272**, 29954-29957.

Bodelon, G., Labrada, L., Martinez-Costas, J., Benavente, J. (2001). The avian reovirus genome segment S1 is a functionally tricistronic gene that expresses one structural and two nonstructural proteins in infected cells. *Virology*, **290**, 181-191.

Bodkin, D. K. and Fields, B. N. (1989). Growth and survival of reovirus in intestinal tissue: role of the L2 and S1 genes. *J. Virol.*, **63**, 1188-1193.

Borsa, J., Sargent, M. D., Lievaart, P. A., Copps, T. P. (1981). Reovirus: evidence for a second step in the intracellular uncoating and transcriptase activation process. *Virology*, **111**, 191-200.

Brown, E. G., Nibert, M. L., Fields, B. N. The L2 gene of reovirus serotype 3 controls the capacity to interfere, accumulate deletions, and establish persistent infection. *In*: Compans RW, Bishop DHL, eds. Double-Stranded RNA Viruses. New York: Elsevier-Biomedical, 1983:275–288.

Chapell, J. D., Goral, M. I., Rodgers, S. E., dePamphilis, C. W., and Dermody, T. S. (1994). Sequence diversity within the reovirus S2 gene: reovirus genes reassort in nature, and their termini are predicted to form a panhandle motif. *J. Virol.*, **68**, 750-756.

Chang, C. T., Zweerink, H. J. (1971). Fate of parental reovirus in infected cell. *Virology.* **46**, 544-555.

Choi, A. H., Paul, R. W., and Lee, P. W. (1990). Reovirus binds to multiple plasma membrane proteins of mouse L fibroblasts. *Virology*, **178**, 316-320.

Chiu, C. J., and Lee, L. H. (1997). Cloning and nucleotide sequencing of the S4 genome segment of avian reovirus S1133. *Arch. Virol.* **142**, 2515-2520.

Cleveland, D. R., Zarbl, H., and Millward, S. (1986). Reovirus guanylyltransferase is L2 gene product lambda 2. *J. Virol.*, **60**, 307-311.

Coombs, K. M. (1996). Identification and characterization of a double-stranded RNA-reovirus temperature-sensitive mutant defective in minor core protein mu2. *J. Virol.*, **70**, 4237-4245.

Coombs, K. M. (1998). Temperature-sensitive mutants of reovirus. *Curr. Top. Microbiol. Immunol.*, **233/I**, 69-107.

Coombs, K. M., Mak, S. C., and Petrycky-Cox, L. D. (1994). Studies of the major reovirus core protein sigma 2: reversion of the assembly-defective mutant *tsC447* is an intragenic process and involves back mutation of Asp-383 to Asn. *J. Virol.*, **68**, 177-186.

Cross, R. K. and Fields, B. N. (1972). Temperature-sensitive mutants of reovirus type 3: studies on the synthesis of viral RNA. *Virology*, **50**, 799-809.

Danis, C., Garzon, S., and Lemay, G. (1992). Further characterization of the *ts453* mutant of mammalian orthoreovirus serotype 3 and nucleotide sequence of the mutated S4 gene. *Virology*, **190**, 494-498.

Dall, D. J., Anzola, J. V., Xu, Z. K., Nuss, D. L. (1990). Structure-specific binding of wound tumor virus transcripts by a host factor: involvement of both terminal nucleotide domains. *Virology,* **179**, 599-608.

Dawe, S., Duncan, R. (2002). The S4 genome segment of baboon reovirus is bicistronic and encodes a novel fusion-associated small transmembrane protein. *J Virol.*, **76**, 2131-2140.

DeLano, W. L. (2003). The PyMOL molecular graphics system. http://www.pymol.org.

Dermody, T. S., Schiff, L. A., Nibert, M. L., Coombs, K. M., Fields, B. N. (1991). The S2 gene nucleotide sequences of prototype strains of the three reovirus serotypes: characterization of reovirus core protein sigma 2. *J Virol.*, **65**:5721-5731.

Drayna, D. and Fields, B. N. (1982a). Activation and characterization of the reovirus transcriptase: genetic analysis. *J. Virol.*, **41**, 110-118.

Drayna, D. and Fields, B. N. (1982b). Genetic studies on the mechanism of chemical and physical inactivation of reovirus. *J. Gen. Virol.*, **63** (Pt 1), 149-159.

Duncan, R. (1996). The low pH-dependent entry of avian reovirus is accompanied by two Specific Cleavages of the Major Outer Capsid Protein mu 2C. *Virology*, **219**, 179-189.

Duncan, R. (1999). Extensive sequence divergence and phylogenetic relationships between the fusogenic and nonfusogenic orthoreoviruses: a species proposal. *Virology,* **260**, 316-328.

Duncan, R., Chen, Z., Walsh, S., Wu, S. (1996). Avian reovirus-induced syncytium formation is independent of infectious progeny virus production and enhances the rate, but is not essential, for virus-induced cytopathology and virus egress. *Virology.* **224**, 453-464.

Ernst, H., Shatkin, A. J. (1985). Reovirus hemagglutinin mRNA codes for two polypeptides in overlapping reading frames. *Proc Natl Acad Sci U S A.*, **82**, 48-52.

Ewing, D. D., Sargent, M. D., Borsa, J. (1985). Switch-on of transcriptase function in reovirus: analysis of polypeptide changes using 2-D gels. *Virology,* **144**, 448-456.

Fahey, J.E., Crawley, J.F. (1954). Studies on chronic respiratory disease of chickens II. Isolation of a virus. *Can. J. Comp. Med.*, **18**, 13-21.

Faust, M., Hastings, K. E., and Millward, S. (1975). m7G5'ppp5'GmptcpUp at the 5' terminus of reovirus messenger RNA. *Nucleic Acids Res.*, **2**, 1329-1343.

Fields, B. N. (1971). Temperature-sensitive mutants of reovirus type 3: features of genetic recombination. *Virology*, **46**, 142-148.

Fields, B. N., Laskov, R., and Scharff, M. D. (1972). Temperature-sensitive mutants of reovirus type 3: studies on the synthesis of viral peptides. *Virology*, **50**, 209-215.

Fields, B. N., Raine, C. S., and Baum, S. G. (1971). Temperature-sensitive mutants of reovirus type 3: defects in viral maturation as studied by immunofluorescence and electron microscopy. *Virology*, **43**, 569-578.

Furuichi, Y., Morgan, M., Muthukrishnan, S., and Shatkin, A. J. (1975). Reovirus messenger RNA contains a methylated, blocked 5'-terminal structure: m-7G(5')ppp(5')G-MpCp-. *Proc. Natl. Acad. Sci. U.S.A*, **72**, 362-366.

Gentsch, J. R. and Hatfield, J. W. (1984). Saturable attachment sites for type 3 mammalian reovirus on murine L cells and human HeLa cells. *Virus Res.*, **1**, 401-414.

Gillies, S., Bullivant, S., and Bellamy, A. R. (1971). Viral RNA polymerases: electron microscopy of reovirus reaction cores. *Science*, **174**, 694-696.

Gomatos, P. J., Prakash, O., Stamatos, N. M. (1981). Small reovirus particle composed solely of sigma NS with specificity for binding different nucleic acids. *J Virol.*, **39**, 115-124.

Gonzalez-Lopez, C., Martinez-Costas, J., Esteban, M., Benavente, J. (2003). Evidence that avian reovirus sigmaA protein is an inhibitor of the double-stranded RNA-dependent protein kinase. *J Gen Virol.*, **84**(Pt 6), 1629-1639

Goodman, J. L., Engel, J. P. (1991). Altered pathogenesis in herpes simplex virus type 1 infection due to a syncytial mutation mapping to the carboxy terminus of glycoprotein B. *J Virol.*, **65**, 1770-1778.

GraphPad InStat Vesion 3. WWW.graphpad.com

Hammond, G. W., Hazelton, P. R., Chuang, I., and Klisko, B. (1981). Improved detection of viruses by electron microscopy after direct ultracentrifuge preparation of specimens. *J. Clin. Microbiol.*, **14**, 210-221.

Hazelton, P. R. and Coombs, K. M. (1995). The reovirus mutant *tsA279* has temperature-sensitive lesions in the M2 and L2 genes: the M2 gene is associated with decreased viral protein production and blockade in transmembrane transport. *Virology,* **207**, 46-58.

Hazelton, P. R. and Coombs, K. M. (1999). The reovirus mutant *tsA279* L2 gene is associated with generation of a spikeless core particle: implications for capsid assembly. *J. Virol.*, **73**, 2298-2308.

Hieronymus, D.R.K., Villegas, P., Kleven, S.H. (1983). Identification and serological differentiation of several reovirus strains isolated from chickens with suspected malabsorption syndrome. *Avian Dis.* **27**, 246-254.

Hooper, J. W. and Fields, B. N. (1996). Role of the mu 1 protein in reovirus stability and capacity to cause chromium release from host cells. *J. Virol.*, **70**, 459-467.

Hsiao, J., Martinez-Costas, J., Benavente, J., Vakharia, V. N. (2002). Cloning, expression, and characterization of avian reovirus guanylyltransferase. *Virology*, **296**, 288-299.

Huismans, H. and Joklik, W. K. (1976). Reovirus-coded polypeptides in infected cells: isolation of two native monomeric polypeptides with affinity for single-stranded and double- stranded RNA, respectively. *Virology,* **70**, 411-424.

Imani, F. and Jacobs, B. L. (1988). Inhibitory activity for the interferon-induced protein kinase is associated with the reovirus serotype 1 sigma 3 protein. *Proc. Natl. Acad. Sci. U.S.A,* **85**, 7887-7891.

Ito, Y., Joklik, W. K. (1972). Temperature-sensitive mutants of reovirus. I. Patterns of gene expression by mutants of groups C, D, and E. *Virology*, **50**, 189-201.

Joklik, W. K. and Roner, M. R. (1995). What reassorts when reovirus genome segments reassort? *J. Biol. Chem.,* **270**, 4181-4184.

Keirstead, N. D., Coombs, K. M. (1998). Absence of superinfection exclusion during asynchronous reovirus infections of mouse, monkey, and human cell lines. *Virus Res.*, **54**, 225-235.

Keroack, M. and Fields, B. N. (1986). Viral shedding and transmission between hosts determined by reovirus L2 gene. *Science,* **232**, 1635-1638.

Kibenge F. S. B., Gwaze G. E., Jones R. C., Chapman A. F. and savage C. E. (1985). Experimental reovirus infection in chickens: observations on early viraemia and virus distribution in bone marrow, liver and enteric tissues. *Avian Pathol.*, **14**, 87-98.

Kibenege, F.S.B., Wilcox, G.E. (1983). Tenosynovitis in chickens. *Vet. Bull.* **53**, 431-443.

Koonin, E. V., Gorbalenya, A. E., and Chumakov, K. M. (1989). Tentative identification of RNA-dependent RNA polymerases of dsRNA viruses and their relationship to positive strand RNA viral polymerases. *FEBS Lett.,* **252**, 42-46.

Kyte, J. and Doolittle, R. F. (1982). A simple method for displaying the hydropathic character of a protein. *J. Mol. Biol.*, **157**, 105-132.

Larson, S. M., Antczak, J. B., Joklik, W. K. (1994). Reovirus exists in the form of 13 particle species that differ in their content of protein sigma 1. *Virology,* **201**, 303-311.

Latorre, P., Kolakofsky, D., Curran, J. (1998). Sendai virus Y proteins are initiated by a ribosomal shunt. *Mol Cell Biol.*, **18**, 5021-5031.

Lemay, G. and Danis, C. (1994). Reovirus lambda 1 protein: affinity for double-stranded nucleic acids by a small amino-terminal region of the protein independent from the zinc finger motif. *J. Gen. Virol.*, **75 (Pt 11)**, 3261-3266.

Leone, G., Mah, D. C., and Lee, P. W. (1991). The incorporation of reovirus cell attachment protein sigma 1 into virions requires the N-terminal hydrophobic tail and the adjacent heptad repeat region. *Virology,* **182**, 346-350.

Lucia-Jandris, P., Hooper, J. W., and Fields, B. N. (1993). Reovirus M2 gene is associated with chromium release from mouse L cells. *J. Virol.*, **67**, 5339-5345.

Mah, D. C., Leone, G., Jankowski, J. M., and Lee, P. W. (1990). The N-terminal quarter of reovirus cell attachment protein sigma 1 possesses intrinsic virion-anchoring function. *Virology,* **179**, 95-103.

Mao, Z., and Joklik, W. K. (1991). Isolation and enzymatic characterization of protein 82, the reovirus guanylyltransferase. *Virology,* **185**, 377-386.

Martinez-Costas, J., Varela, R, Benavente, J. (1995). Endogenous enzymatic activities of the avian reovirus S1133: identification of the viral capping enzyme. *Virology*, **206**, 1017-1026.

Martinez-Costas, J., Grande, A., Varela, R., Garcia-Martinez, C., Benavente, J. (1997). Protein architecture of avian reovirus S1133 and identification of the cell attachment protein. *J Virol.*, **71**, 59-64.

Martinez-Costas, J., Gonzalez-Lopez, C., Vakharia, V. N., Benavente, J. (2000). Possible involvement of the double-stranded RNA-binding core protein sigmaA in the resistance of avian reovirus to interferon. *J Virol.*, **74**, 1124-1131.

Matsuhisa, T., Joklik, W. K. (1974). Temperature-sensitive mutants of reovirus. V. Studies on the nature of the temperature-sensitive lesion of the group C mutant *ts447. Virology*, **60**, 380-389.

Mbisa, J. L., Becker, M. M., Zou, S., Dermody, T. S., Brown, E. G. (2000). Reovirus mu2 protein determines strain-specific differences in the rate of viral inclusion formation in L929 cells. *Virology*, **272**, 16-26.

McCarthy, C. (2001). Chromas© version 2.13. School of Health Science, Griffith University, Gold Coast Campus, Southport, Queensland, Australia.

Meanger, J., Wickramasinghe, R., Enriquez, C. E, Wilcox, G. E. (1999). Association between the sigma C protein of avian reovirus and virus-induced fusion of cells. *Arch Virol.*, **144**, 193-197.

Mendez, I. I.; Hermann, L. L.; Hazelton, P. R.; Coombs, K. M. (2000). A comparative analysis of freon substitutes in the purification of reovirus and calicivirus. *J. Virol. Methods*, **90**, 59-67.

Miller, C. L., Broering, T. J., Parker, J. S., Arnold, M. M., and Nibert, M. L. (2003). Reovirus sigma NS protein localizes to inclusions through an association requiring the mu NS amino terminus. *J Virol.*, **77**, 4566-4576.

Morgan, E. M. and Zweerink, H. J. (1975). Characterization of transcriptase and replicase particles isolated from reovirus-infected cells. *Virology*, **68**, 455-466.

Morozov, S. Y. (1989). A possible relationship of reovirus putative RNA polymerase to polymerases of positive-strand RNA viruses. *Nucleic Acids Res.*, **17**, 5394

Ni, Y., Kemp, M. C. (1992). Strain-specific selection of genome segments in avian reovirus coinfections. *J Gen Virol.*, **73 (Pt 12),** 3107-3113.

Ni, Y., Kemp, M. C. (1994). Subgenomic S1 segments are packaged by avian reovirus defective interfering particles having an S1 segment deletion. *Virus Res.,*; **32,**: 329-342.

Ni, Y., and Ramig, R. F. (1993). Characterization of avian reovirus-induced cell fusion: The role of viral structural proteins. *Virology*, **194**, 705-714.

Nibert, M. L. and Fields, B. N. (1992). A carboxy-terminal fragment of protein mu 1/mu 1C is present in infectious subvirion particles of mammalian reoviruses and is proposed to have a role in penetration. *J. Virol.*, **66**, 6408-6418.

Nibert, M. L., Margraf, R. L., and Coombs, K. M. (1996). Nonrandom segregation of parental alleles in reovirus reassortants. *J. Virol.*, **70**, 7295-7300.

Nibert, M. L., and Schiff, L. A. (2001). Reoviruses and their replication. *In* "Fields Virology" 4th ed. (Knipe, D. M., and Howley, P. M. Eds) VOl 2, pp 1679-1728. Lippincott, Williams and Wilkins: Philadelphia, USA.

Noble, S. and Nibert, M. L. (1997). Core protein mu2 is a second determinant of nucleoside triphosphatase activities by reovirus cores. *J. Virol.*, **71**, 7728-7735

Nonoyama, M., Graham, A. F. (1970). Appearance of defective virions in clones of reovirus. *J Virol* **6**, 693–694.

Nonoyama, M., Watanabe, Y., Graham, A. F. (1970). Defective virions of reovirus. *J Virol* **6**, 226–236.

Nonoyama, M., Millward, S., Graham, A. F. (1974). Control of transcription of the reovirus genome. *Nucleic Acids Res.*, **1**, 373-385.

Nuss, D. L., Summers, D. (1984). Variant dsRNAs associated with transmission-defective isolates of wound tumor virus represent terminally conserved remnants of genome segments. *Virology.* **133**, 276-288.

O'Hara, D., Patrick, M., Cepica, D., Coombs, K. M., Duncan, R. (2001). Avian reovirus major mu-class outer capsid protein influences efficiency of productive macrophage infection in a virus strain-specific manner. *J Virol.* **75**, 5027-5035.

Patrick, M. (2001). The generation and characterization of avian reovirus temperature sensitive mutants. M.Sc. thesis. University of Manitoba, Winnipeg, Manitoba, Canada.

Patrick, M., Duncan, R., Coombs, K. M. (2001). Generation and genetic characterization of avian reovirus temperature-sensitive mutants. *Virology.* **284**, 113-122

Park, B. H., Matuschke, B., Lavi, E., Gaulton, G. N. (1994). A point mutation in the env gene of a murine leukemia virus induces syncytium formation and neurologic disease. *J Virol.* **68**, 7516-7524.

Paul, R. W., Choi, A. H., and Lee, P. W. (1989). The alpha-anomeric form of sialic acid is the minimal receptor determinant recognized by reovirus. *Virology,* **172**, 382-385.

Prevelige, P. E. Jr. (1998). Inhibiting virus-capsid assembly by altering the polymerisation pathway. *Trends Biotechnol.* **16**, 61-65.

Ramig, R. F., Mustoe, T. A., Sharpe, A. H., and Fields, B. N. (1978). A genetic map of reovirus. II. Assignment of the double-stranded RNA- negative mutant groups C, D, and E to genome segments. *Virology,* **85**, 531-534.

Ramig, R. F., Ward, R. L., Ramig, R. F., Ward, R. L. (1991). *Adv Virus Res.* **39**, 163-207

Reinisch, K. M., Nibert, M. L., and Harrison, S. C. (2000). Structure of the reovirus core at 3.6 Å resolution. *Nature,* **404**, 960-967.

Robertson, M. D., and Wilcox, G. E. (1986). Avian reovirus. *vet. Bull.* **56**, 759-766.

Roner, M. R., Sutphin, L. A., and Joklik, W. K. (1990). Reovirus RNA is infectious. *Virology,* **179**, 845-852.

Roner, M. R., Neplioueν, I., Sherry, B., Joklik, W. K. (1997). Construction and characterization of a reovirus double temperature-sensitive mutant. *Proc Natl Acad Sci U S A.* **94**, 6826-6830.

Sato, H., Orenstein, J., Dimitrov, D., Martin, M. (1992). Cell-to-cell spread of HIV-1 occurs within minutes and may not involve the participation of virus particles. *Virology.* **186**, 712-724.

Schuerch, A. R., Matsuhisa, T., Joklik, W. K. (1974). Temperature-sensitive mutants of reovirus. VI. Mutant *ts* 447 and *ts* 556 particles that lack either one or two genome RNA segments. *Intervirology* **3**, 336–346.

Seliger, L. S., Zheng, K., and Shatkin, A. J. (1987). Complete nucleotide sequence of reovirus L2 gene and deduced amino acid sequence of viral mRNA guanylyltransferase. *J. Biol. Chem.*, **262**, 16289-16293.

Shapouri, M. R., Arella, M., Silim, A. (1996). Evidence for the multimeric nature and cell binding ability of avian reovirus sigma 3 protein. *J Gen Virol.* **77** (Pt 6), 1203-1210.

Shapouri, M. R., Kane, M., Letarte, M., Bergeron, J., Arella, M., Silim, A. (1995). Cloning, sequencing and expression of the S1 gene of avian reovirus. *J Gen Virol.* **76**, 1515-1520.

Shapouri, M. R., Arella, M., Silim, A. (1996). Evidence for the multimeric nature and cell binding ability of avian reovirus sigma 3 protein. *J Gen Virol.* **77**, 1203-1210.

Shapouri, M. R. S., Frenette, D., Larochelle, R., Arella, M., and Silim, A. (1996). Characterization of monoclonal antibodies against avian reovirus strain S1133. *Avian Pathol.* **25**, 57-67.

Shatkin, A. J., Furuichi, Y., LaFiandra, A. J., and Yamakawa, M. (1983). Double-stranded RNA viruses. In Compans, R.W.; Bishop, D. H. L. eds. Elsevier, New York pp:43-54.

Sherry, B., Torres, J., Blum, M. A. (1998). Reovirus induction of and sensitivity to beta interferon in cardiac myocyte cultures correlate with induction of myocarditis and are determined by viral core proteins. *J Virol.* **72**, 1314-1323

Shing, M. and Coombs, K. M. (1996). Assembly of the reovirus outer capsid requires mu 1/sigma 3 interactions which are prevented by misfolded sigma 3 protein in temperature-sensitive mutant *tsG453*. *Virus Res.*, **46**, 19-29.

Shmulevitz, M., Duncan, R. (2000). A new class of fusion-associated small transmembrane (FAST) proteins encoded by the non-enveloped fusogenic reoviruses. *EMBO J.* 19, 902-912.

Shmulevitz, M., Yameen, Z., Dawe, S., Shou, J., O'Hara, D., Holmes, I., Duncan, R. (2002). Sequential partially overlapping gene arrangement in the tricistronic S1 genome segments of avian reovirus and Nelson Bay reovirus: implications for translation initiation. *Virol.* **76**, 609-618.

Shmulevitz, M., Salsman, J., Duncan, R. (2003). Palmitoylation, membrane-proximal basic residues, and transmembrane glycine residues in the reovirus p10 protein are essential for syncytium formation *J Virol.* **77**, 9769-9779.

Silverstein, S. C., Astell, C., Levin, D. H, Schonberg, M., Acs, G. (1972). The mechanisms of reovirus uncoating and gene activation in vivo. *Virology.* **47**, 797-806.

Skup, D., Millward, S. (1980). Reovirus-induced modification of cap-dependent translation in infected L cells. *Proc Natl Acad Sci U S A.* **77**, 152-156.

Spandidos, D. A., Krystal, G., Graham, A. F. (1976). Regulated transcription of the genomes of defective virions and temperature-sensitive mutants of reovirus. *J Virol.* **18**, 7-19.

Starnes, M. C. and Joklik, W. K. (1993). Reovirus protein lambda 3 is a poly(C)-dependent poly(G) polymerase. *Virology,* **193**, 356-366.

Sturzenbecker, L. J., Nibert, M., Furlong, D., Fields, B. N. (1987). Intracellular digestion of reovirus particles requires a low pH and is an essential step in the viral infectious cycle. *J Virol.* **61**, 2351-2361.

Tang, D., Strong, J. E., and Lee, P. W. (1993). Recognition of the epidermal growth factor receptor by reovirus. *Virology,* **197**, 412-414.

Theophilos, M. B., Huang, J. A., Holmes, I. H. (1995). Avian reovirus sigma C protein contains a putative fusion sequence and induces fusion when expressed in mammalian cells. *Virology*, **208,** 678-684.

Tosteson, M. T., Nibert, M. L., and Fields, B. N. (1993). Ion channels induced in lipid bilayers by subvirion particles of the nonenveloped mammalian reoviruses. *Proc. Natl. Acad. Sci. U.S.A,* **90**, 10549-10552.

Touris-Otero, F., Martinez-Costas, J., Vakharia, V. N., and Benavente, J. (2004). Avian reovirus nonstructural protein microNS forms viroplasm-like inclusions and recruits protein sigmaNS to these structures. *Virology*, **319**, 94-106.

van Regenmortel, M. H. V., Fauquet, C. M., Bishop, D. H. L., Carstens, E. B., Ester, M. K., Lemon, S. M., Maniloff, J., Mayo, M. A., McGeoch, D. J., Pringle, C. R., and Wickner, R. B. (eds.) (2000). Reoviridae. In *Virus Taxonomy: Seventh report of the International Committee on Taxonomy of Viruses.* Academic Press, San Diego, CA. pp: 395-480.

Varela, R., Benavente, J. (1994). Protein coding assignment of avian reovirus strain S1133. *J Virol.* **68**, 6775-6777.

Watanabe, Y., Millward, S., Graham, A. F. (1968). Regulation of transcription of the Reovirus genome. *J Mol Biol.* **36**, 107-23.

Weiner, H. L., Powers, M. L., Fields, B. N. (1980). Absolute linkage of virulence and central nervous system cell tropism of reoviruses to viral hemagglutinin. *J Infect Dis.* **141**, 609-616.

White, J. M. (1990). Viral and cellular membrane fusion proteins. *Annu. Rev. Physiol.* **52**, 675-679.

Wickramasinghe R, Meanger J, Enriquez C, Wilcox G. (1993). Avian reovirus proteins associated with neutralization of virus infectivity. *Virology* **194,** 688–696.

Wiener, J. R., Bartlett, J. A., and Joklik, W. K. (1989a). The sequences of reovirus serotype 3 genome segments M1 and M3 encoding the minor protein mu 2 and the major nonstructural protein mu NS, respectively. *Virology*, **169**, 293-304.

Wiener, J. R., T. McLaughlin, W. K. Joklik. (1989b). The sequences of the S2 genome segments of reovirus serotype 3 and of the dsRNA-negative mutant *ts447*. *Virology*. **170**, 340-341.

Wilcox, G. E., Compans, R. W., Wilcox, G. E., Compans, R. W. (1982). *Virology*. **123,** 312-322.

Xu, Z. K., Anzola, J. V., Nalin, C. M., Nuss, D. L. (1989). The 3'-terminal sequence of a wound tumor virus transcript can influence conformational and functional properties associated with the 5'-terminus. *Virology*. **170**, 511-522.

Yin, H. S., Shieh, H. K., Lee, L. H. (1997). Characterization of the double-stranded RNA genome segment S3 of avian reovirus. *J Virol Methods*. **67**, 93-101.

Yin, H. S., Shien, J. H., Lee, L. H. (2000). Synthesis in Escherichia coli of avian reovirus core protein varsigmaA and its dsRNA-binding activity. *Virology* **266**, 33-41.

Yin, H. S., Yu, P. S., and Lee, L. H. (2002). Evidence of nucleotidyl phosphatase activity associated with core protein σA of avian reovirus S1133. *Virology* **293**, 379-385.

Yin, P., Cheang, M., and Coombs, K. M. (1996). The M1 gene is associated with differences in the temperature optimum of the transcriptase activity in reovirus core particles. *J. Virol.*, **70**, 1223-1227.

Zarbl, H., Skup, S., and Millward, S. (1980). Reovirus progeny subviral particles synthesize uncapped mRNA. *J. Virol.*, **34**, 497-505.

Zarbl, H. and Millward, S. (1983). The Reoviridae. 107-196.

Zou, S. and Brown, E. G. (1992). Identification of sequence elements containing signals for replication and encapsidation of the reovirus M1 genome segment. *Virology,* **186**, 377-388.

Zou, S., Brown, E. G. (1996). Stable expression of the reovirus mu2 protein in mouse L cells complements the growth of a reovirus *ts* mutant with a defect in its M1 gene. *Virology*. **217**, 42-48.

Zweerink, H. J., Ito, Y., and Matsuhisa, T. (1972). Synthesis of reovirus double-stranded RNA within virion like particles. *Virology*, **50**, 349-358.

Zweerink, H. J., Morgan, E. M., Skyler, J. S. (1976). Reovirus morphogenesis: characterization of subviral particles in infected cells. *Virology*. **73**, 442-453.